

Search for new physics in events with opposite-sign leptons, jets, and missing transverse energy in pp collisions at $\sqrt{s} = 7$ TeV

The CMS Collaboration*

Abstract

A search is presented for physics beyond the standard model (BSM) in final states with a pair of opposite-sign isolated leptons accompanied by jets and missing transverse energy. The search uses LHC data recorded at a center-of-mass energy $\sqrt{s} = 7$ TeV with the CMS detector, corresponding to an integrated luminosity of approximately 5 fb^{-1} . Two complementary search strategies are employed. The first probes models with a specific dilepton production mechanism that leads to a characteristic kinematic edge in the dilepton mass distribution. The second strategy probes models of dilepton production with heavy, colored objects that decay to final states including invisible particles, leading to very large hadronic activity and missing transverse energy. No evidence for an event yield in excess of the standard model expectations is found. Upper limits on the BSM contributions to the signal regions are deduced from the results, which are used to exclude a region of the parameter space of the constrained minimal supersymmetric extension of the standard model. Additional information related to detector efficiencies and response is provided to allow testing specific models of BSM physics not considered in this paper.

Submitted to the Journal of High Energy Physics

1 Introduction

In this paper we describe a search for physics beyond the standard model (BSM) in events containing a pair of opposite-sign leptons, jets, and missing transverse energy (E_T^{miss}), in a sample of proton-proton collisions at a center-of-mass energy of 7 TeV. The data sample was collected with the Compact Muon Solenoid (CMS) detector [1] at the Large Hadron Collider (LHC) in 2011 and corresponds to an integrated luminosity of 4.98 fb^{-1} . This is an update and extension of a previous analysis performed with a data sample of 34 pb^{-1} collected in 2010 [2].

The BSM signature in this search is motivated by three general considerations. First, new particles predicted by BSM physics scenarios are expected to be heavy in most cases, since they have so far eluded detection. Second, BSM physics signals may be produced with large cross section via the strong interaction, resulting in significant hadronic activity. Third, astrophysical evidence for dark matter suggests [3–6] that the mass of weakly-interacting massive particles is of the order of the electroweak symmetry breaking scale. Such particles, if produced in proton-proton collisions, could escape detection and give rise to an apparent imbalance in the event transverse energy. The analysis therefore focuses on the region of high E_T^{miss} . An example of a specific BSM scenario is provided by R-parity conserving supersymmetric (SUSY) models, in which the colored squarks and gluinos are pair-produced and subsequently undergo cascade decays, producing jets and leptons [7, 8]. These cascade decays may terminate in the production of the lightest SUSY particle (LSP), often the lightest neutralino, which escapes detection and results in large E_T^{miss} . This LSP is a candidate for a dark matter weakly-interacting massive particle. Another BSM scenario which may lead to similar signatures is the model of universal extra dimensions (UED) [9].

The results reported in this paper are part of a broad program of BSM searches in events with jets and E_T^{miss} , classified by the number and type of leptons in the final state. Here we describe a search for events containing an opposite-sign isolated lepton pair in addition to jets and E_T^{miss} . We reconstruct electrons and muons, which provide a clean signature with low background. In addition, we reconstruct τ leptons in their hadronic decay modes to improve the sensitivity to models with enhanced coupling to third generation particles. Complementary CMS searches with different final states have already been reported, for example in Refs. [10, 11]. Results from the ATLAS collaboration in this final state using approximately $1\text{--}2 \text{ fb}^{-1}$ have been reported in Refs. [12, 13].

The analysis strategy is as follows. In order to select dilepton events, we use a preselection based on that of the CMS top quark pair ($t\bar{t}$) cross section measurement in the dilepton channel [14]; the details of this preselection are presented in Section 3. Reasonable agreement is found between the observed yields in data and the predictions from standard model (SM) Monte Carlo (MC) simulation. Two complementary search strategies are pursued, which are optimized for different experimental signatures. The first strategy is a search for a kinematic edge [15] in the dilepton ($ee, \mu\mu$) mass distribution. This is a characteristic feature of SUSY models in which the same-flavor opposite-sign leptons are produced via the decay $\tilde{\chi}_2^0 \rightarrow \tilde{\ell}\ell \rightarrow \tilde{\chi}_1^0 \ell^+ \ell^-$, where $\tilde{\chi}_2^0$ is the next-to-lightest neutralino, $\tilde{\chi}_1^0$ is the lightest neutralino, and $\tilde{\ell}$ is a slepton. The second strategy is a search for an excess of events with dileptons accompanied by very large hadronic activity and E_T^{miss} . We perform counting experiments in four signal regions with requirements on these quantities to suppress the $t\bar{t}$ background, and compare the observed yields with the predictions from a background estimation technique based on data control samples, as well as with SM and BSM MC expectations. These two search approaches are complementary, since the dilepton mass edge search is sensitive to new physics models that have lower E_T^{miss} and hadronic energy, while the counting experiments do not as-

sume a specific dilepton production mechanism and are also sensitive to BSM scenarios that produce lepton pairs with uncorrelated flavor.

No specific BSM physics scenario, e.g. a particular SUSY model, has been used to optimize the search regions. In order to illustrate the sensitivity of the search, a simplified and practical model of SUSY breaking, the constrained minimal supersymmetric extension of the standard model (CMSSM) [16, 17] is used. The CMSSM is described by five parameters: the universal scalar and gaugino mass parameters (m_0 and $m_{1/2}$, respectively), the universal trilinear soft SUSY breaking parameter A_0 , the ratio of the vacuum expectation values of the two Higgs doublets ($\tan\beta$), and the sign of the Higgs mixing parameter μ . Throughout the paper, four CMSSM parameter sets, referred to as LM1, LM3, LM6, and LM13 [18], are used to illustrate possible CMSSM yields. The parameter values defining LM1 (LM3, LM6, LM13) are $m_0 = 60$ (330, 85, 270) GeV, $m_{1/2} = 250$ (240, 400, 218) GeV, $\tan\beta = 10$ (20, 10, 40), $A_0 = 0$ (0, 0, -553) GeV; all four parameter sets have $\mu > 0$. These four scenarios are beyond the exclusion reach of previous searches performed at the Tevatron and LEP, and are chosen here because they produce events containing opposite-sign leptons and may lead to a kinematic edge in the dilepton mass distribution. These four scenarios serve as common benchmarks to facilitate comparisons of sensitivity among different analyses.

2 The CMS detector

The central feature of the CMS detector is a superconducting solenoid, 13 m in length and 6 m in diameter, which provides an axial magnetic field of 3.8 T. Within the field volume are several particle detection systems. Charged particle trajectories are measured by silicon pixel and silicon strip trackers covering $|\eta| < 2.5$ in pseudorapidity, where $\eta = -\ln[\tan\theta/2]$ with θ the polar angle of the particle trajectory with respect to the counterclockwise proton beam direction. A crystal electromagnetic calorimeter and a brass/scintillator hadron calorimeter surround the tracking volume, providing energy measurements of electrons, photons and hadronic jets. Muons are identified and measured in gas-ionization detectors embedded in the steel return yoke outside the solenoid. The detector is nearly hermetic, allowing energy balance measurements in the plane transverse to the beam direction. The first level of the CMS trigger system, composed of custom hardware processors, uses information from the calorimeters and muon detectors to select, in less than $1\ \mu\text{s}$, the most interesting events. The High Level Trigger processor farm further decreases the event rate from around 100 kHz to around 300 Hz, before data storage. Event reconstruction is performed with the particle-flow (PF) algorithm [19], which is used to form a mutually exclusive collection of reconstructed particles (muons, electrons, photons, charged and neutral hadrons) by combining tracks and calorimeter clusters. A more detailed description of the CMS detector can be found elsewhere [1].

3 Event Selection

The following samples of simulated events are used to guide the design of the analysis. These events are generated with either PYTHIA 6.4.22 [20], MADGRAPH 4.4.12 [21], or POWHEG [22] MC event generators using the CTEQ 6.6 parton density functions [23]. The $t\bar{t}$, $W + \text{jets}$, and VV ($V = W, Z$) samples are generated with MADGRAPH, with parton showering simulated by PYTHIA using the Z2 tune [24]. The single-top samples are generated with POWHEG. The Drell-Yan (DY) sample is generated using a mixture of MADGRAPH (for events with dilepton invariant mass above 50 GeV) and PYTHIA (for events with dilepton invariant mass in the range 10–50 GeV), and includes decays to the $\tau\tau$ final state. The signal events are simulated using

PYTHIA. The detector response in these samples is then simulated with a GEANT4 model [25] of the CMS detector. The MC events are reconstructed and analyzed with the same software as is used to process collision data. Due to the varying instantaneous LHC luminosity, the mean number of interactions in a single beam crossing increased over the course of the data-taking period to a maximum of about 15. In the MC simulation, multiple proton-proton interactions are simulated by PYTHIA and superimposed on the hard collision, and the simulated samples are reweighted to describe the distribution of reconstructed primary vertices in data [26]. The simulated sample yields are normalized to an integrated luminosity of 4.98 fb^{-1} using next-to-leading order (NLO) cross sections.

Events in data are selected with a set of ee , $e\mu$, $\mu\mu$, $e\tau$, and $\mu\tau$ double-lepton triggers. Since the online reconstruction of hadronic- τ decays (τ_h) is difficult, τ_h triggers are intrinsically prone to high rates. Therefore, for the analysis with two τ_h only, we use specialized triggers that rely on significant hadronic activity H_T , quantified by the scalar sum of online jet transverse energies with $p_T > 40 \text{ GeV}$, and E_T^{miss} as well as the presence of two τ_h . The efficiencies for events containing two leptons passing the analysis selection to pass at least one of these triggers are measured to be approximately $1.00^{+0.00}_{-0.02}$, 0.95 ± 0.02 , 0.90 ± 0.02 , 0.80 ± 0.05 , 0.80 ± 0.05 and 0.90 ± 0.05 for ee , $e\mu$, $\mu\mu$, $e\tau_h$, $\mu\tau_h$ and $\tau_h\tau_h$ triggers, respectively. In the following, the simulated sample yields for the light lepton channels are weighted by these trigger efficiencies. For the τ_h channels the trigger simulation is applied to the MC simulation and then a correction is applied based on the measured data and MC efficiencies for these triggers.

Because leptons produced in the decays of low-mass particles, such as hadrons containing b and c quarks, are nearly always inside jets, they can be suppressed by requiring the leptons to be isolated in space from other particles that carry a substantial amount of transverse momentum. The details of the lepton isolation measurement are given in Ref. [14]. In brief, a cone is constructed of size $\Delta R \equiv \sqrt{(\Delta\eta)^2 + (\Delta\phi)^2} = 0.3$ around the lepton momentum direction. The lepton relative isolation is then quantified by summing the transverse energy (as measured in the calorimeters) and the transverse momentum (as measured in the silicon tracker) of all objects within this cone, excluding the lepton, and dividing by the lepton transverse momentum. The resulting quantity is required to be less than 0.15, rejecting the large background arising from QCD production of jets.

The τ_h decays are reconstructed with the PF algorithm and identified with the hadrons-plus-strips (HPS) algorithm, which considers candidates with one or three charged pions and up to two neutral pions [27]. As part of the τ_h identification procedure, loose isolation is applied for the τ_h final states. Isolated electrons and muons can be misidentified as τ_h candidates. For this reason τ_h candidates are required to fail electron selections and not to match a muon signature in the muon system.

Events with two opposite-sign isolated leptons are selected. At least one of the leptons must have $p_T > 20 \text{ GeV}$, both must have $p_T > 10 \text{ GeV}$, and the electrons (muons) must have $|\eta| < 2.5$ ($|\eta| < 2.4$). Electrons in the range $1.44 < |\eta| < 1.57$ are excluded. In events containing a τ_h candidate, both leptons must satisfy $p_T > 20 \text{ GeV}$ and $|\eta| < 2.1$, where the acceptance requirement is tightened so that the τ_h decay products are contained in the tracking detector in a manner that is consistent with the requirements of the triggers used for these events. In events with more than one opposite-sign pair that satisfy the selection requirements, the two oppositely-signed leptons with highest p_T are chosen. Events with an ee or $\mu\mu$ pair with invariant mass of the dilepton system between 76 GeV and 106 GeV or below 12 GeV are removed, in order to suppress $Z/\gamma^* \rightarrow \ell\ell$ events, as well as low-mass dilepton resonances. Events containing two electrons, two muons, or an electron and a muon are referred to as the “light lepton channels,”

Table 1: Summary of event preselection requirements applied in the light lepton channels, hadronic- τ channels, and the dilepton mass edge search of Section 4. The leading (trailing) lepton is the one with highest (second highest) p_T . The requirements on jet multiplicity, scalar sum of jet transverse energies (H_T), missing transverse energy (E_T^{miss}), and dilepton mass are also indicated.

Requirement	light leptons	hadronic- τ	edge search
leading lepton	e or μ , $p_T > 20$ GeV	e, μ , or τ_h , $p_T > 20$ GeV	e or μ , $p_T > 20$ GeV
trailing lepton	e or μ , $p_T > 10$ GeV	e, μ , or τ_h , $p_T > 20$ GeV	e or μ , $p_T > 10$ GeV
jet multiplicity	$n_{\text{jets}} \geq 2$	$n_{\text{jets}} \geq 2$	$n_{\text{jets}} \geq 2$
H_T	$H_T > 100$ GeV	$H_T > 100$ GeV	$H_T > 300$ GeV
E_T^{miss}	$E_T^{\text{miss}} > 50$ GeV	$E_T^{\text{miss}} > 100$ GeV	$E_T^{\text{miss}} > 150$ GeV
dilepton mass	veto $76 < m_{ee}, m_{\mu\mu} < 106$ GeV	-	-

while events with at least one τ_h are referred to as “hadronic- τ channels.”

The PF objects are clustered to form jets using the anti- k_T clustering algorithm [28] with the distance parameter of 0.5. We apply p_T - and η -dependent corrections to account for residual effects of nonuniform detector response, and impose quality criteria to reject jets that are consistent with anomalous detector noise. We require the presence of at least two jets with transverse momentum of $p_T > 30$ GeV and $|\eta| < 3.0$, separated by $\Delta R > 0.4$ from leptons passing the analysis selection. For each event the scalar sum of transverse energies of selected jets H_T must exceed 100 GeV. The E_T^{miss} is defined as the magnitude of the vector sum of the transverse momenta of all PF objects, and we require $E_T^{\text{miss}} > 50$ GeV ($E_T^{\text{miss}} > 100$ GeV) in the light lepton (hadronic- τ) channels.

The event preselection requirements are summarized in Table 1. The data yields and corresponding MC predictions after this event preselection are given in Table 2 (light leptons) and Table 3 (hadronic- τ). For the light lepton channels, the normalization of the simulated yields has been scaled based on studies of $Z \rightarrow \ell\ell$ in data and in MC simulation, to account for effects of lepton selection and trigger efficiency and to match the integrated luminosity. As expected, the MC simulation predicts that the sample passing the preselection is dominated by lepton pair final states from $t\bar{t}$ decays (dilepton $t\bar{t}$). The data yield is in good agreement with the prediction, within the systematic uncertainties of the integrated luminosity (2.2%) and $t\bar{t}$ cross section determination (12%) [29–31]. The yields for the LM1, LM3, LM6, and LM13 benchmark scenarios are also quoted.

4 Search for a Kinematic Edge

We search for a kinematic edge (end-point) in the dilepton mass distribution for same-flavor (SF) light-lepton events, i.e., ee or $\mu\mu$ lepton pairs. Such an edge is a characteristic feature of, for example, SUSY scenarios in which the opposite-sign leptons are produced via the decay $\tilde{\chi}_2^0 \rightarrow \tilde{\ell}\bar{\ell} \rightarrow \tilde{\chi}_1^0 \ell^+ \ell^-$. The model of UED can lead to a similar signature with different intermediate particles. In case of a discovery such a technique offers one of the best possibilities for model-independent constraints of the SUSY mass parameters [15].

In contrast, for the dominant background $t\bar{t}$ as well as other SM processes such as WW and $DY \rightarrow \tau\tau$, the two lepton flavors are uncorrelated, and the rates for SF and opposite-flavor (OF) $e\mu$ lepton pairs are therefore the same. Hence we can search for new physics in the SF final

Table 2: Data yields and MC predictions in the light lepton channels after preselection, using the quoted NLO production cross sections σ . The $t\bar{t} \rightarrow \ell^+\ell^-$ contribution corresponds to dilepton $t\bar{t}$ with no $W \rightarrow \tau$ decays, $t\bar{t} \rightarrow \ell^\pm\tau^\mp/\tau^+\tau^-$ refers to dilepton $t\bar{t}$ with at least one $W \rightarrow \tau$ decay, and $t\bar{t} \rightarrow \ell^\pm + \text{jets/hadrons}$ includes all other $t\bar{t}$ decay modes. The quoted cross sections for these processes include the relevant branching fractions. The LM points are benchmark SUSY scenarios, which are defined in the text. The MC uncertainties include the statistical component, the uncertainty in the integrated luminosity, and the dominant uncertainty from the $t\bar{t}$ cross-section determination. The data yield is in good agreement with the MC prediction, but the latter is not used explicitly in the search. The difference between the $ee + \mu\mu$ versus $e\mu$ yields is due to the rejection of ee and $\mu\mu$ events with an invariant mass consistent with that of the Z boson.

Sample	σ [pb]	ee	$\mu\mu$	$e\mu$	Total
$t\bar{t} \rightarrow \ell^+\ell^-$	7	1466 ± 179	1872 ± 228	4262 ± 520	7600 ± 927
$t\bar{t} \rightarrow \ell^\pm\tau^\mp/\tau^+\tau^-$	9	303 ± 37	398 ± 49	889 ± 108	1589 ± 194
$t\bar{t} \rightarrow \ell^\pm + \text{jets/hadrons}$	141	50 ± 6.2	15 ± 1.9	90 ± 11	155 ± 19
$DY \rightarrow \ell\ell$	16677	193 ± 11	237 ± 13	312 ± 15	741 ± 26
WW	43	55 ± 1.7	66 ± 1.9	151 ± 3.8	272 ± 6.5
WZ	18	13 ± 0.4	15 ± 0.4	25 ± 0.6	53 ± 1.3
ZZ	5.9	2.6 ± 0.1	3.3 ± 0.1	3.3 ± 0.1	9.1 ± 0.3
Single top	102	95 ± 3.1	120 ± 3.7	278 ± 7.3	492 ± 12
W + jets	96648	47 ± 11	9.8 ± 4.6	59 ± 12	117 ± 16
Total MC		2224 ± 224	2735 ± 281	6069 ± 643	11029 ± 1137
Data		2333	2873	6184	11390
LM1	6.8	272 ± 8.3	342 ± 9.7	166 ± 5.7	780 ± 20
LM3	4.9	107 ± 3.7	125 ± 4.1	181 ± 5.5	413 ± 11
LM6	0.4	20 ± 0.6	23 ± 0.7	26 ± 0.8	69 ± 1.7
LM13	9.8	138 ± 6.6	157 ± 7.0	334 ± 12	629 ± 19

Table 3: Data yields and MC predictions in hadronic- τ channels after preselection, using the quoted NLO production cross sections σ . Diboson backgrounds comprise WW, WZ and ZZ events. The sum of simulated events is also split into events with a generated τ_h (MC, genuine τ_h) and events with a misidentified τ_h (MC, misidentified τ_h); the two contributions are equally important. The channel with two τ_h decays is not presented because the trigger is not efficient in the preselection region, due to the large H_T requirement. The uncertainty indicated represents both statistical and systematic components.

Sample	σ [pb]	$e\tau_h$	$\mu\tau_h$	Total
$DY \rightarrow \ell\ell$	16677	51 ± 12	47 ± 11	98 ± 22
$t\bar{t}$	157.5	165 ± 47	205 ± 58	370 ± 105
Diboson	66.9	11 ± 2.0	10.8 ± 1.9	22 ± 3.6
Single top	102	7.2 ± 2.6	8.1 ± 2.7	15 ± 4.8
Σ MC, genuine τ_h		146 ± 39	167 ± 44	313 ± 83
Σ MC, misidentified τ_h		89 ± 24	103 ± 27	191 ± 51
Total MC		235 ± 62	271 ± 72	505 ± 134
Data		215	302	517
LM1	6.8	36 ± 6.7	46 ± 6.8	82 ± 9.8
LM3	4.9	28 ± 6.0	18 ± 4.6	46 ± 7.6
LM6	0.4	2.8 ± 1.1	4.2 ± 1.3	7.0 ± 1.7
LM13	9.8	90 ± 11	118 ± 12	208 ± 16

state and model the backgrounds using events in the OF final state. Thus the $t\bar{t}$ background shape is extracted from events with OF lepton pairs, and a fit is performed to the dilepton mass distribution in events with SF lepton pairs.

In order to be sensitive to BSM physics over the full dilepton mass spectrum, events with a dilepton invariant mass $m_{\ell\ell}$ consistent with that of the Z boson are not rejected. This increases the DY contribution, which is compensated by an increase in the $E_T^{\text{miss}} > 150$ GeV requirement (see Table 1). We then proceed to search for a kinematic edge in the signal region defined as $H_T > 300$ GeV. The invariant mass distributions of SF and OF lepton pairs are in good agreement with each other (see Fig. 1). A fit is performed to the dilepton mass distribution with three candidate signal shapes, over a range of values on the position of the kinematic edge.

The flavor-uncorrelated background, as a function of the invariant mass $m_{\ell\ell}$, is parameterized as:

$$B(m_{\ell\ell}) = m_{\ell\ell}^a e^{-bm_{\ell\ell}}, \quad (1)$$

where $a \approx 1.4$ describes the rising edge and $b \approx 0.002$ dominates the long exponential tail on the right hand side of the background shape; these parameters are extracted from the fit to data.

We parametrize the signal shape with an edge model for two subsequent two-body decays, according to:

$$S(m_{\ell\ell}) = \frac{1}{\sqrt{2\pi}\sigma_{ll}} \int_0^{m_{\text{max}}} dy y^\alpha e^{-\frac{(m_{\ell\ell}-y)^2}{2\sigma_{ll}^2}}. \quad (2)$$

For $\alpha = 1$ this function describes a triangle convoluted with a Gaussian, which accounts for detector resolution effects. The resolution parameters for electrons σ_{ee} and muons $\sigma_{\mu\mu}$ are constrained with simulation. The DY contribution, found to be negligible as seen in Fig. 1, is modelled by a Breit-Wigner function with the mass and width parameters fixed at the Z boson mass and width, convoluted with a Gaussian function to account for the detector resolution.

We perform a simultaneous, extended, unbinned maximum likelihood fit to the distribution of dilepton mass for events containing ee , $\mu\mu$ (signal, DY and background model), and $e\mu$ pairs (background model only). The value of the kinematic edge position m_{max} is varied, and the fit is performed for each value of this parameter. The shape parameters of the flavor-uncorrelated background that are free in the fit are assumed to be common in all categories, and the yields of signal (n_S), DY (n_{DY}) and background (n_B) in these three categories are constrained using the ratio of muon to electron selection efficiencies $R_{\mu e} = 1.11 \pm 0.05$. This quantity is evaluated using studies of DY events in data and in MC simulation.

The fit is performed in the signal region $H_T > 300$ GeV and $E_T^{\text{miss}} > 150$ GeV. The SF events overlaid with the signal plus background fit, and the flavor-uncorrelated shape overlaid with OF events, are shown in Fig. 1. The results of the fit are displayed for a value of the kinematic edge position $m_{\text{max}} = 280$ GeV, where the largest excess is observed. The local significance is 2.1σ including statistical and systematic uncertainties. However, a correction for the look-elsewhere effect [32] reduces the global significance to 0.7σ . The extracted signal yield including statistical uncertainty ($n_S = 11_{-5.7}^{+6.5}$) at this point is consistent with the background-only hypothesis, and we derive a 95% confidence level upper limit of $n_S < 23$ events for this kinematic edge position. No evidence for a kinematic edge feature is observed in the dilepton mass distribution.

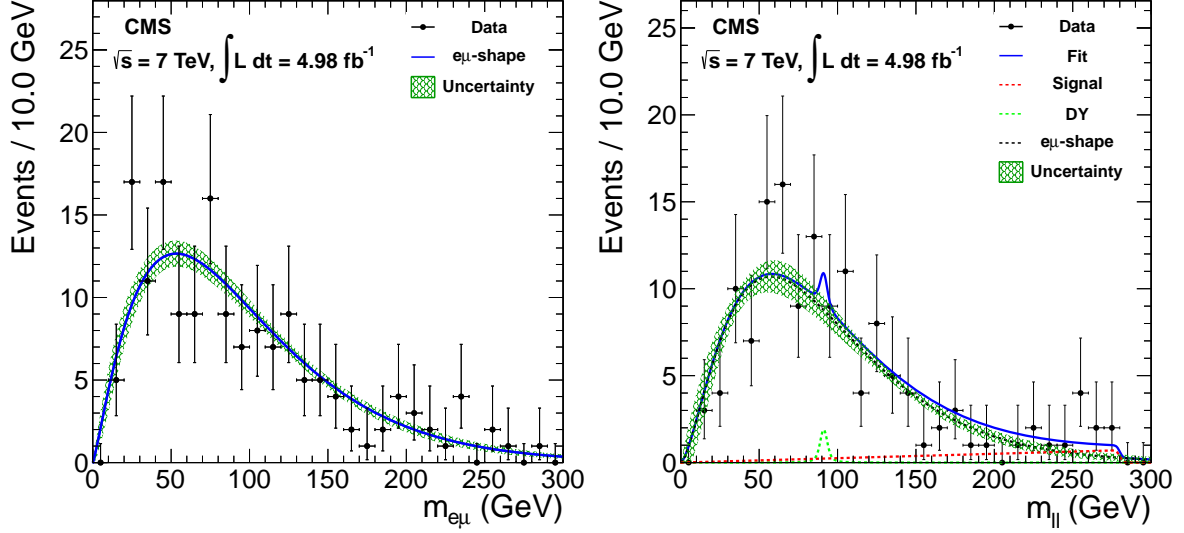


Figure 1: Distribution of events (black points) and the results of the maximum likelihood fit (blue curve) to the dilepton mass distribution for events containing $e\mu$ lepton pairs (left), and ee and $\mu\mu$ lepton pairs (right) in the signal region $H_T > 300$ GeV and $E_T^{\text{miss}} > 150$ GeV, that suppresses DY contributions almost completely. The signal hypothesis for a value of the kinematic edge position $m_{\text{max}} = 280$ GeV, corresponding to the largest local excess, is displayed. The shaded band represents the shape uncertainty of the background model.

5 Counting Experiments

We next proceed to search for an excess of events containing lepton pairs accompanied by large E_T^{miss} and H_T . To look for possible BSM contributions, we define four signal regions that reject all but $\sim 0.1\%$ of the dilepton $t\bar{t}$ events, by adding the following requirements:

- high- E_T^{miss} signal region : $E_T^{\text{miss}} > 275$ GeV, $H_T > 300$ GeV,
- high- H_T signal region : $E_T^{\text{miss}} > 200$ GeV, $H_T > 600$ GeV,
- tight signal region : $E_T^{\text{miss}} > 275$ GeV, $H_T > 600$ GeV,
- low- H_T signal region : $E_T^{\text{miss}} > 275$ GeV, $125 < H_T < 300$ GeV.

The signal regions are indicated in Fig. 2. These signal regions are tighter than the one used in Ref. [2] since with the larger data sample the tighter signal regions allow us to explore phase space farther from the core of the SM distributions. The observed and estimated yields in the high- E_T^{miss} , high- H_T , and tight signal regions are used in the CMSSM exclusion limit in Section 7. The low- H_T region has limited sensitivity to CMSSM models that tend to produce low- p_T leptons, since the large E_T^{miss} and low H_T requirements lead to the requirement of large dilepton p_T . However, the results of this region are included to extend the sensitivity to other models that produce high- p_T leptons.

5.1 Light lepton channels

The dominant background in the signal regions is dilepton $t\bar{t}$ production. This background is estimated using a technique based on data control samples, henceforth referred to as the dilepton transverse momentum ($p_T(\ell\ell)$) method. This method is based on the fact [33] that in dilepton $t\bar{t}$ events the p_T distributions of the charged leptons (electrons and muons) and neutrinos are related, since each lepton-neutrino pair is produced in the two-body decay of the

W boson. This relation depends on the polarization of the W bosons, which is well understood in top quark decays in the SM [34–36], and can therefore be reliably accounted for. In dilepton $t\bar{t}$ events, the values of $p_T(\ell\ell)$ and the transverse momentum of the dineutrino system ($p_T(\nu\nu)$) are approximately uncorrelated on an event-by-event basis. We thus use the observed $p_T(\ell\ell)$ distribution to model the $p_T(\nu\nu)$ distribution, which is identified with E_T^{miss} . Thus, we predict the background in a signal region S defined by requirements on E_T^{miss} and H_T using the yield in a region S' defined by replacing the E_T^{miss} requirement by the same requirement on $p_T(\ell\ell)$.

To suppress the DY contamination to the region S' , we increase the E_T^{miss} requirement to $E_T^{\text{miss}} > 75$ GeV for SF events and subtract off the small residual DY contribution using the $R_{\text{out/in}}$ technique [14] based on control samples in data. This technique derives, from the observed DY yield in the Z mass region, the expected yield in the complementary region using the ratio $R_{\text{out/in}}$ extracted from MC simulation. Two corrections are applied to the resulting prediction, following the same procedure as in Ref. [2]. The first correction accounts for the fact that we apply minimum requirements to E_T^{miss} in the preselection but there is no corresponding requirement on $p_T(\ell\ell)$. Since the E_T^{miss} and $p_T(\ell\ell)$ are approximately uncorrelated in individual dilepton $t\bar{t}$ events, the application of the E_T^{miss} requirement decreases the normalization of the $p_T(\ell\ell)$ spectrum without significantly altering the shape. Hence, we apply correction factors K , which are extracted from data as $K = 1.6 \pm 0.1, 1.6 \pm 0.4, 1.6 \pm 0.4,$ and 1.9 ± 0.1 for the high- E_T^{miss} , high- H_T , tight, and low- H_T signal regions, respectively. The uncertainty in K is dominated by the statistical component. The second correction factor K_C accounts for the W polarization in $t\bar{t}$ events, as well as detector effects such as hadronic energy scale; this correction is extracted from MC and is $K_C = 1.6 \pm 0.5, 1.4 \pm 0.2, 1.7 \pm 0.4,$ and 1.0 ± 0.4 for the four respective regions. The uncertainty in K_C is dominated by MC sample statistics and by the 7.5% uncertainty in the hadronic energy scale in this analysis.

Backgrounds from DY are estimated from data with the $R_{\text{out/in}}$ technique, which leads to an estimated DY contribution consistent with zero. Backgrounds from processes with two vector bosons as well as electroweak single top quark production are negligible compared with those from dilepton $t\bar{t}$ decays.

Backgrounds in which one or both leptons do not originate from electroweak decays (misidentified leptons) are assessed using the “tight-to-loose” (TL) ratio (R_{TL}) method of Ref. [14]. A misidentified lepton is a lepton candidate originating from within a jet, such as a lepton from semileptonic b or c decays, a muon from a pion or kaon decay-in-flight, a pion misidentified as an electron, or an unidentified photon conversion. The results of the tight-to-loose ratio method confirm the MC expectation that the misidentified lepton contribution is small compared to the dominant backgrounds. Estimates of the contributions to the signal region from QCD multijet events, with two misidentified leptons, and in $W + \text{jets}$, with one misidentified lepton in addition to the lepton from the decay of the W, are derived separately. The contributions are found to be less than $\sim 10\%$ of the total background in the signal regions, which is comparable to the contribution in the control regions used to estimate the background from the $p_T(\ell\ell)$ method. We therefore assign an additional systematic uncertainty of 10% on the background prediction from the $p_T(\ell\ell)$ method due to misidentified leptons.

As a validation of the $p_T(\ell\ell)$ method in a region that is dominated by background, the $p_T(\ell\ell)$ method is also applied in a control region by restricting H_T to be in the range 125–300 GeV. Here the predicted background yield is 95 ± 16 (stat) ± 40 (syst) events with $E_T^{\text{miss}} > 200$ GeV, including the systematic uncertainties in the correction factors K and K_C , and the observed yield is 59 events.

The data are displayed in the plane of E_T^{miss} vs. H_T in Fig. 2. The predicted and observed E_T^{miss}

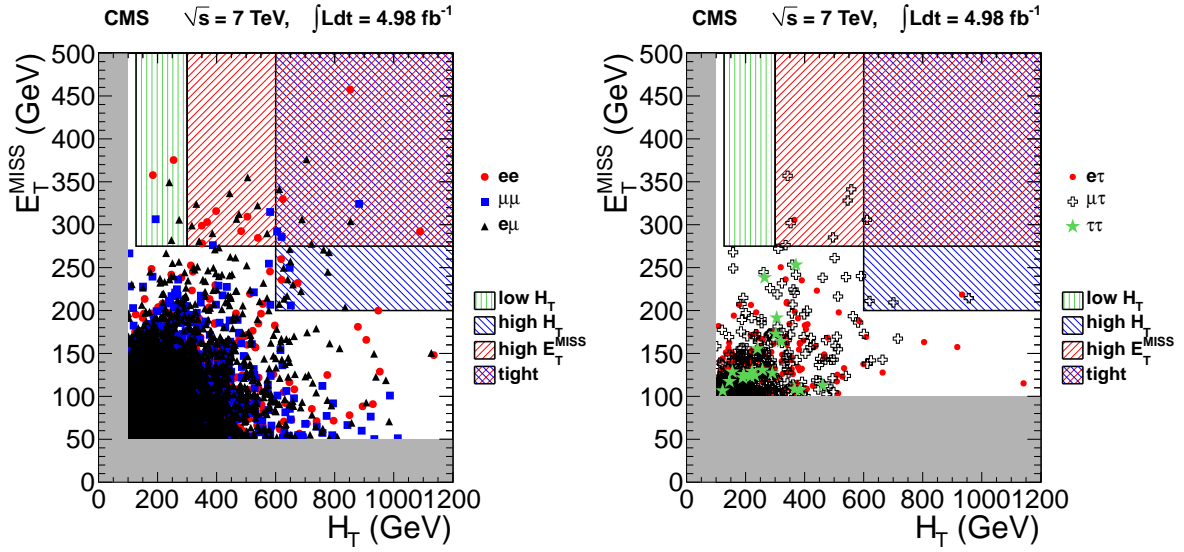


Figure 2: Distributions of E_T^{miss} vs. H_T for data in the light lepton channels (left) and hadronic- τ channels (right). The signal regions are indicated as hatched regions. The solid gray region is excluded at the preselection level.

distributions are displayed in Fig. 3. A summary of these results is presented in Table 4. The SF and OF observed yields in the signal regions are quoted separately, since many SUSY models lead to enhanced production of SF lepton pairs. For all signal regions, the observed yield is consistent with the predictions from MC and from the background estimate based on data. No evidence for BSM contributions to the signal regions is observed in the light lepton channels.

5.2 Hadronic- τ channels

In the hadronic- τ channels the background has two components of similar importance, events with a genuine lepton pair from dilepton $t\bar{t}$ production and events from semi-leptonic $t\bar{t}$ and $W + \text{jets}$ production with a misidentified τ_h . Backgrounds are estimated separately with techniques based on data control samples. Other very small contributions from DY and diboson production with genuine lepton pairs (“MC irreducible”) are estimated from simulation.

The background with genuine lepton pairs is predicted by extending the $p_T(\ell\ell)$ method. To translate the background prediction in the ee , $e\mu$, and $\mu\mu$ channels into a prediction for the $e\tau_h$, $\mu\tau_h$, and $\tau_h\tau_h$ channels, a third correction factor is used. This correction, $K_\tau = 0.10 \pm 0.01$ for all signal regions, is estimated from simulation and accounts for the different lepton acceptances (~ 0.75), branching fractions (~ 0.56), and efficiencies (~ 0.24) in hadronic- τ channels. This procedure predicts the yield of the dilepton $t\bar{t}$ background with genuine hadronic τ decays.

The background with a reconstructed τ_h originating from a misidentified jet or a secondary decay is determined using a tight-to-loose ratio for τ_h candidates measured in a dijet dominated data sample, defined as $H_T > 200 \text{ GeV}$ and $E_T^{\text{miss}} < 20 \text{ GeV}$. Tight candidates are defined as those that pass the full τ_h selection criteria. For the definition of loose candidates, the HPS isolation criterion is replaced by a looser requirement. The loose isolation requirement removes any H_T dependence of the tight-to-loose ratio; thus the measurement can be extrapolated to the signal regions.

To determine the number of expected events including jets misidentified as τ_h candidates in the signal region, the identification requirements for one τ_h are loosened. The obtained yields are

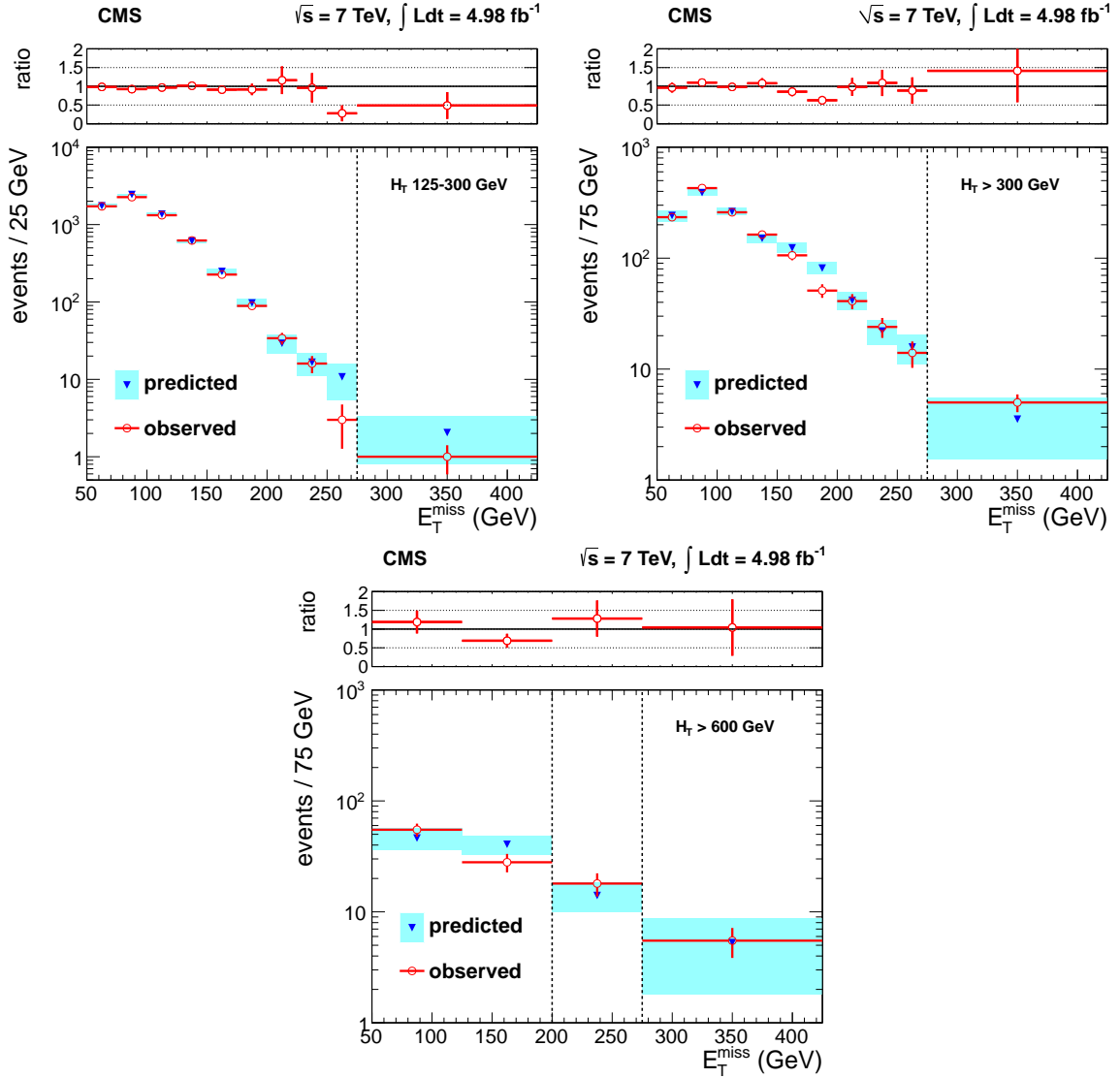


Figure 3: The observed E_T^{miss} distributions (red points) and E_T^{miss} distributions predicted by the $p_T(\ell\ell)$ method (blue points with shaded uncertainty bands) in data for the region $125 < H_T < 300$ GeV (upper left), $H_T > 300$ GeV (upper right), and $H_T > 600$ GeV (bottom). The uncertainty bands on the predicted E_T^{miss} distribution are statistical, and also include systematic uncertainties for points in the signal regions, to the right of the vertical dashed line. The ratio of data to predicted background is also included. The error bars include the full uncertainties on the data and predicted background.

Table 4: Summary of results in the light lepton channels. The total SM MC expected yields (MC prediction), observed same-flavor (SF), opposite-flavor (OF), and total yields in the signal regions are indicated, as well as the predicted yields from the $p_T(\ell\ell)$ estimate. The the expected contributions from three benchmark SUSY scenarios are also quoted. The first uncertainty on the $p_T(\ell\ell)$ method prediction is statistical and the second is systematic; the systematic uncertainty is discussed in the text. The non-SM yield upper limit (UL) is a 95% CL upper limit on the signal contribution.

	high E_T^{miss}	high H_T	tight	low H_T
MC prediction	30 ± 1.2	31 ± 0.9	12 ± 0.6	4.2 ± 0.3
SF yield	15	11	6	3
OF yield	15	18	5	3
Total yield	30	29	11	6
$p_T(\ell\ell)$ prediction	$21 \pm 8.9 \pm 8.0$	$22 \pm 7.5 \pm 6.9$	$11 \pm 5.8 \pm 3.8$	$12 \pm 4.9 \pm 5.7$
Observed UL	26	23	11	6.5
Expected UL	21	19	11	8.6
LM1	221 ± 5.1	170 ± 4.5	106 ± 3.5	6.2 ± 0.9
LM3	79 ± 2.4	83 ± 2.5	44 ± 1.8	2.3 ± 0.4
LM6	35 ± 0.6	33 ± 0.5	26 ± 0.5	0.6 ± 0.1
LM13	133 ± 5.5	113 ± 5.2	65 ± 3.9	4.1 ± 0.9

multiplied by the probability P_{TL} that a misidentified τ_h candidate passes the tight τ_h selection:

$$P_{TL}(p_T, \eta) = \frac{R_{TL}(p_T, \eta)}{1 - R_{TL}(p_T, \eta)}.$$

A summation over P_{TL} evaluated for all τ_h candidates that pass the loose selection but not the tight selection gives the final background prediction in each signal region.

The method is validated in $t\bar{t}$ simulation, where the agreement between the predicted and true yields is within 15%. We correct for a 5% bias observed in the simulation, and assign a 15% systematic uncertainty on the background prediction from the tight-to-loose ratio based on the agreement between prediction and observation in simulation and additional control samples in data.

The results in the four signal regions are summarized in Table 5. The low- H_T region includes only $e\tau_h$ and $\mu\tau_h$ channels, because the $\tau_h\tau_h$ trigger is inefficient in this region. In the high- E_T^{miss} region the $\tau_h\tau_h$ trigger is not fully efficient and an efficiency correction of 3% is applied to MC simulation. Good agreement between predicted and observed yields is observed. No evidence for BSM physics is observed in the hadronic- τ channels.

The results of observed yields and predicted backgrounds in all signal regions for different lepton categories are summarized in Fig. 4.

6 Acceptance and Efficiency Systematic Uncertainties

The acceptance and efficiency, as well as the systematic uncertainties in these quantities, depend on the process. For some of the individual uncertainties, it is reasonable to quote values based on SM control samples with kinematic properties similar to the SUSY benchmark mod-

Table 5: Summary of the observed and predicted yields in the four signal regions for hadronic- τ channels. The first indicated error is statistical and the second is systematic; the systematic uncertainties on the R_{TL} ratio and $p_T(\ell\ell)$ method predictions are discussed in the text. The non-SM yield upper limit is a 95% CL upper limit on the signal contribution in each signal region.

	high E_T^{miss}	high H_T	tight	low H_T
Σ MC, genuine τ_h	5.8 ± 2.3	3.7 ± 1.6	2.0 ± 1.2	0.4 ± 0.2
Σ MC, misidentified τ_h	1.4 ± 0.5	2.8 ± 1.3	0.2 ± 0.1	0.2 ± 0.1
Total MC	7.1 ± 2.5	6.5 ± 2.3	2.2 ± 1.2	0.7 ± 0.3
$p_T(\ell\ell)$ prediction	$2.1 \pm 0.9 \pm 0.8$	$2.2 \pm 0.8 \pm 0.9$	$1.1 \pm 0.6 \pm 0.4$	$1.2 \pm 0.5 \pm 0.4$
R_{TL} prediction	$5.1 \pm 1.7 \pm 0.8$	$3.6 \pm 1.4 \pm 0.5$	$2.7 \pm 1.3 \pm 0.4$	$< 0.9@95\%CL$
MC irreducible	$1.3 \pm 0.5 \pm 0.2$	$0.7 \pm 0.3 \pm 0.1$	$0.2 \pm 0.1 \pm 0.1$	$0.1 \pm 0.1 \pm 0.1$
Σ predictions	$8.5 \pm 2.0 \pm 1.1$	$6.5 \pm 1.6 \pm 1.0$	$4.0 \pm 1.4 \pm 0.6$	$1.3 \pm 0.5 \pm 0.5$
Total yield	8	5	1	0
Observed UL	7.9	6.2	3.7	3.1
Expected UL	8.1	7.2	5.7	3.9
LM1	32 ± 11	14 ± 6.1	8.1 ± 4.2	–
LM3	11 ± 4.2	11 ± 5.1	8.0 ± 4.9	–
LM6	4.5 ± 1.5	5.1 ± 1.6	4.2 ± 1.6	0.4 ± 0.4
LM13	69 ± 17	52 ± 8.2	39 ± 9.8	–

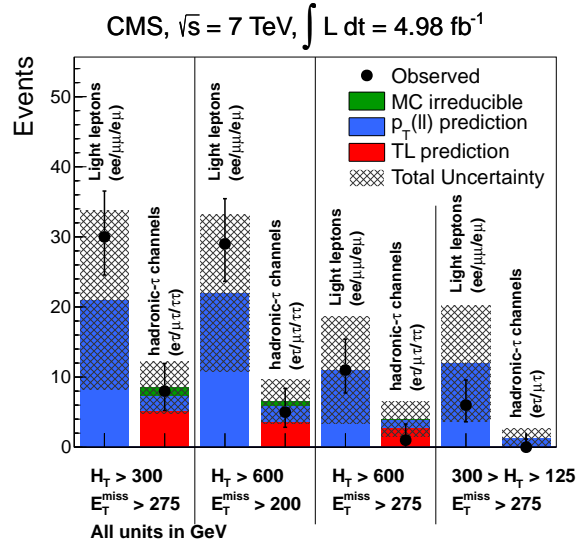


Figure 4: Summary of the background predictions from tight-to-loose ratio, $p_T(\ell\ell)$ -method and MC, and observed yields in the signal regions.

els. For others that depend strongly on the kinematic properties of the event, the systematic uncertainties must be quoted model-by-model.

The systematic uncertainty in the lepton acceptance consists of two parts: the trigger efficiency uncertainty, and the identification and isolation uncertainty. The trigger efficiency for two leptons of $p_T > 10$ GeV, with one lepton of $p_T > 20$ GeV is measured using samples of $Z \rightarrow \ell\ell$, with an uncertainty of 2%. The simulated events reproduce the lepton identification and isolation efficiencies measured in data using samples of $Z \rightarrow \ell\ell$ within 2% for lepton $p_T > 15$ GeV and within 7% (5%) for electrons (muons) in the range $p_T = 10$ –15 GeV. The uncertainty of the trigger efficiency (5%) of the τ_h triggers is estimated with the tag-and-probe method [37]. The τ_h identification efficiency uncertainty is estimated to be 6% from an independent study using a tag-and-probe technique on $Z \rightarrow \tau\tau$ events. This is further validated by obtaining a $Z \rightarrow \tau\tau$ enhanced region showing consistency between simulation and data. Another significant source of systematic uncertainty is associated with the jet and E_T^{miss} energy scale. The impact of this uncertainty is final-state dependent. Final states characterized by very large hadronic activity and E_T^{miss} are less sensitive than final states where the E_T^{miss} and H_T are typically close to the minimum requirements applied to these quantities. To be more quantitative, we have used the method of Ref. [14] to evaluate the systematic uncertainties in the acceptance for three benchmark SUSY points. The energies of jets in this analysis are known to within 7.5%; the correction accounting for the small difference between the hadronic energy scales in data and MC is not applied [38].

The uncertainty on the LM1 signal efficiency in the region $H_T > 300$ GeV, $E_T^{\text{miss}} > 150$ GeV used to search for the kinematic edge is 6%. The uncertainties for the four benchmark SUSY scenarios in the signal regions used for the counting experiments of Section 5 are displayed in Table 6. The uncertainty in the integrated luminosity is 2.2%.

Table 6: Summary of the relative uncertainties in the signal efficiency due to the jet and E_T^{miss} scale, for the four benchmark SUSY scenarios in the signal regions used for the counting experiments of Section 5.

Signal Model	high E_T^{miss}	high H_T	tight	low H_T
LM1	22%	33%	40%	19%
LM3	26%	34%	42%	18%
LM6	11%	15%	19%	10%
LM13	26%	31%	40%	14%

7 Limits on New Physics

7.1 Search for a kinematic edge

An upper limit on the signal yield is extracted from the fit to the dilepton mass distribution, assuming the triangular shape ($\alpha = 1$) of Eq. (2). The 95% CL upper limit is extracted using a hybrid frequentist-bayesian CL_S method [39], including uncertainties in the background model, resolution model and Z -boson yield. We scan the position of the kinematic edge m_{max} and extract a signal yield upper limit for each value, as shown in Fig. 5. The extracted upper limits on n_S vary in the range 5–30 events; these upper limits do not depend strongly on the choice of signal shape parameter when using two different shapes specified by a concave ($\alpha = 4$) and convex curvature (hatched band).

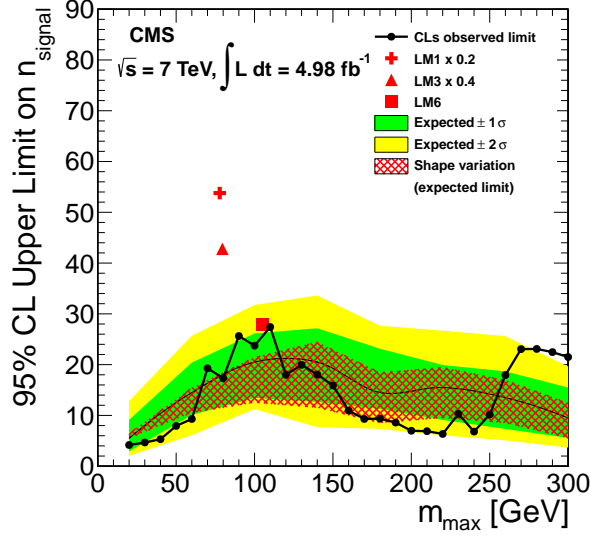


Figure 5: A CL_S 95% CL upper limit on the signal yield n_S as a function of the endpoint in the invariant mass spectrum m_{\max} assuming a triangular shaped signal (black dots and thick line). The hatched band shows the variation of the expected limit (thin line) assuming two alternate signal shapes, with the alternative expected limits corresponding to the boundary of the hatched band. The SUSY benchmark scenarios LM1, LM3 and LM6 are shown with their expected yields and theoretical positions of the corresponding kinematic dilepton mass edges. The LM1 (LM3) yield is scaled to 20% (40%) of its nominal yield. At LM3 and LM6 a three-body decay is present; thus the shape of the kinematic edge is only approximately triangular.

7.2 Search for an excess of events with large E_T^{miss} and H_T

In this section we use the results of the search for events with light leptons accompanied by large E_T^{miss} and H_T reported in Section 5 to exclude a region of the CMSSM parameter space. The exclusion is performed using multiple, exclusive signal regions based on the high- E_T^{miss} , high- H_T , and tight signal regions, divided into three non-overlapping regions in the E_T^{miss} vs. H_T plane. The results are further divided between the SF and OF final states in order to improve the sensitivity to models with correlated dilepton production leading to an excess of SF events, yielding a total of six signal bins, as summarized in Table 7. The use of multiple, disjoint signal regions improves the sensitivity of this analysis to a specific BSM scenario. The predicted backgrounds in the SF and OF final states are both equal to half of the total predicted background, because the $t\bar{t}$ events produce equal SF and OF yields. The inputs to the upper limit calculation are the expected background yields and uncertainties from the $p_T(\ell\ell)$ method, the expected signal yields and uncertainties from MC simulation, and the observed data yields in these six regions. The exclusion is performed with the CL_S method. In the presence of a signal, the $p_T(\ell\ell)$ background estimate increases due to signal events populating the control regions. To correct for this effect, for each point in the CMSSM parameter space this expected increase is subtracted from the signal yields in our search regions.

The SUSY particle spectrum is calculated using SOFTSUSY [40], and the signal events are generated at leading order (LO) with PYTHIA 6.4.22. We use NLO cross sections, obtained with the program PROSPINO [41]. Experimental uncertainties from luminosity, trigger efficiency, and lepton selection efficiency are constant across the CMSSM plane, while the uncertainty from the hadronic energy scale is assessed separately at each CMSSM point taking into account the bin-to-bin migration of signal events. The variation in the observed and expected limits due to

Table 7: Summary of results in the light lepton channels used for the CMSSM exclusion of Section 7. Details are the same as in Table 4 except that these results are divided into three non-overlapping regions defined by $E_T^{\text{miss}} > 275$ GeV, H_T 300–600 GeV (SR1), $E_T^{\text{miss}} > 275$ GeV, $H_T > 600$ GeV (SR2, same as the “tight” signal region), and $E_T^{\text{miss}} 200$ –275 GeV, $H_T > 600$ GeV (SR3). The regions are further divided between same-flavor (SF) and opposite-flavor (OF) lepton pairs.

	SR1	SR2	SR3
SF yield	9	6	5
OF yield	10	5	13
$p_T(\ell\ell)$ prediction	$5.7 \pm 5.1 \pm 2.8$	$5.3 \pm 4.1 \pm 1.9$	$5.6 \pm 3.4 \pm 2.1$

the theoretical uncertainties, including renormalization and factorization scale, parton density functions (PDFs), and the strong coupling strength α_S [42], are indicated in Fig. 6 as separate exclusion contours. These results significantly extend the sensitivity of our previous results [2]. The LEP-excluded regions are also indicated; these are based on searches for sleptons and charginos [43].

8 Additional Information for Model Testing

Other models of new physics in the dilepton final state can be constrained in an approximate way by simple generator-level studies that compare the expected number of events in the data sample corresponding to an integrated luminosity of 4.98 fb^{-1} with the upper limits from Section 7. The key ingredients of such studies are the kinematic requirements described in this paper, the lepton efficiencies, and the detector responses for H_T and E_T^{miss} . The trigger efficiencies for events containing ee , $e\mu$ or $\mu\mu$ lepton pairs are 100%, 95%, and 90%, respectively. For $e\tau_h$, and $\mu\tau_h$ the efficiency is $\sim 80\%$ [37]. The trigger used for $\tau_h\tau_h$ final states has an efficiency of 90%.

We evaluate the light lepton, hadronic- τ , E_T^{miss} , and H_T selection efficiencies using the LM6 benchmark model, but these efficiencies do not depend strongly on the choice of model. Jets at the generator-level are approximated as quarks or gluons produced prior to the parton showering step satisfying $p_T > 30$ GeV and $|\eta| < 3$. Generator-level leptons are required to satisfy $p_T > 10$ GeV and $|\eta| < 2.5$ and not to overlap with a generator-level jet within $\Delta R < 0.4$. For generator level τ_h the visible decay products are required to satisfy the tighter $p_T > 20$ GeV and $|\eta| < 2.1$ selection. The generator-level E_T^{miss} is the absolute value of the vector sum of the transverse momenta of invisible particles, e.g., neutrinos and lightest supersymmetric particles. The lepton selection efficiencies as a function of generator-level p_T are displayed in Fig. 7. The efficiency dependence can be parameterized as a function of p_T as

$$f(p_T) = \epsilon_\infty \{\text{erf}[(p_T - C)/\sigma]\} + \epsilon_C \{1 - \text{erf}[(p_T - C)/\sigma]\}, \quad (3)$$

where erf indicates the error function, ϵ_∞ gives the value of the efficiency plateau at high momenta, C is equal to 10 GeV, ϵ_C gives the value of the efficiency at $p_T = C$, and σ describes how fast the transition is. The parameterization is summarized in Table 8 for electrons, muons, and taus.

The E_T^{miss} and H_T selection efficiencies are displayed in Fig. 8 as a function of the generator-level quantities. These efficiencies are parameterized using the function:

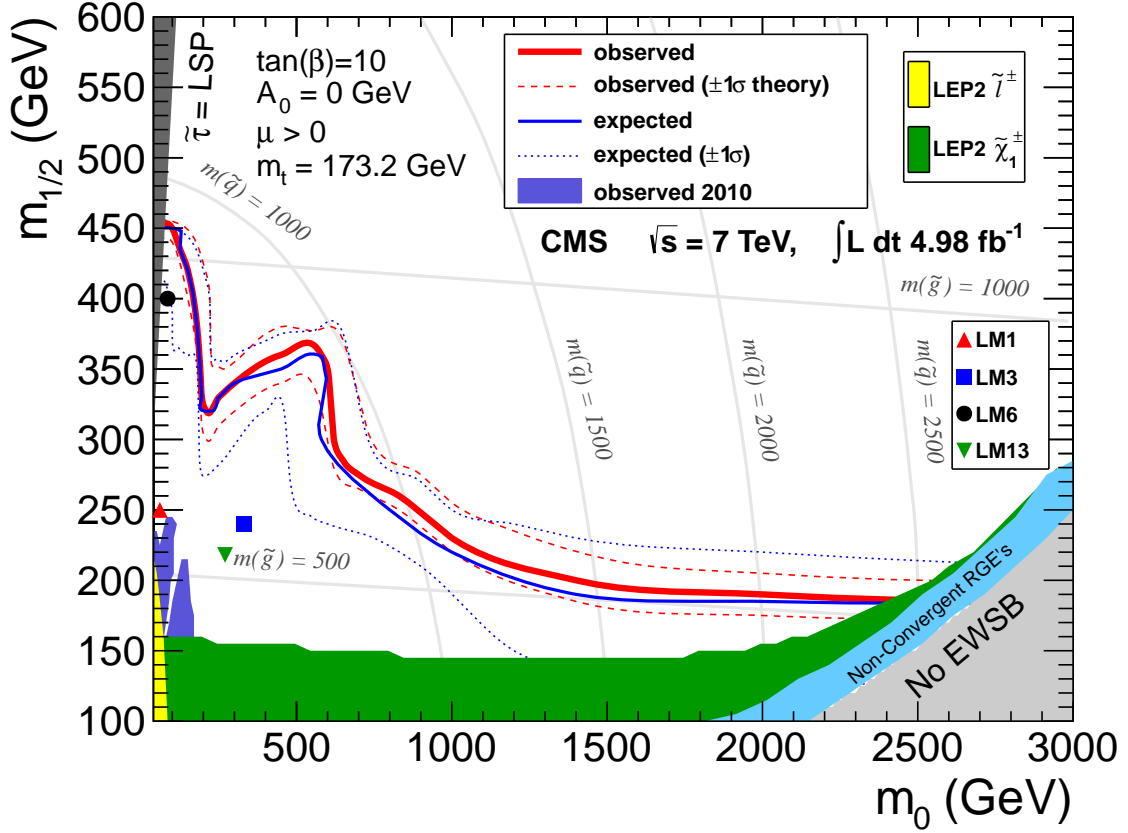


Figure 6: The observed 95% CL exclusion contour (solid thick red line), the expected exclusion contour (solid thin blue line), the variation in the observed exclusion from the variation of PDF, renormalization and factorization scales, and α_s theoretical uncertainties (dashed red lines), the $\pm 1\sigma$ uncertainty in the median expected exclusion (dotted blue lines), and the observed exclusion contour based on 34 pb^{-1} 2010 data in the opposite-sign dilepton channel (dark blue shaded region), in the CMSSM $(m_0, m_{1/2})$ plane for $\tan \beta = 10$, $A_0 = 0 \text{ GeV}$ and $\mu > 0$. The area below the red curve is excluded by this search. Exclusion limits obtained from the LEP experiments are presented as shaded areas in the plot. The thin grey lines correspond to constant squark and gluino masses. The LM benchmark SUSY scenarios are also indicated. The LM3 and LM13 benchmark scenarios have values of $\tan \beta$ and/or A_0 that differ from 10 and 0 GeV, respectively, but both are also excluded by the results of this search; see the text of Section 1 for the full definitions of these scenarios.

Table 8: Values of the fitted parameters in Eq. (3) for the lepton selection efficiencies of Fig. 7.

Parameter	e	μ	τ_h
C	10 GeV	10 GeV	10 GeV
ϵ_∞	0.78	0.89	0.44
ϵ_C	0.34	0.62	0.31
σ	18 GeV	30 GeV	13 GeV

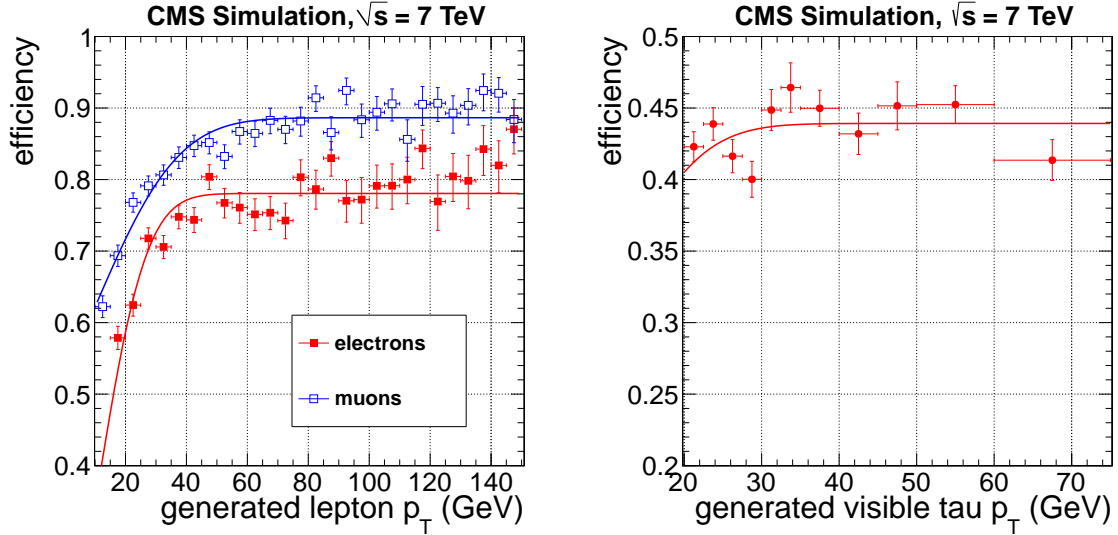


Figure 7: The efficiency to pass the light lepton (left), and hadronic- τ (right) selection as a function of the generator-level p_T (visible τ_h p_T). These efficiencies are calculated using the LM6 MC benchmark.

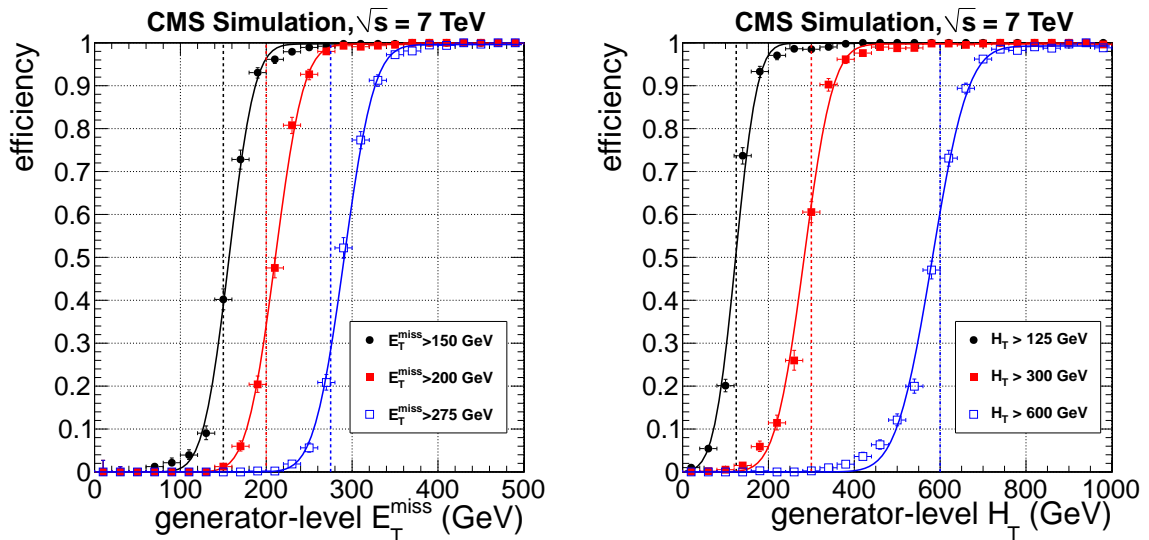


Figure 8: The efficiency to pass the signal region E_T^{miss} (left), and H_T (right) requirements as a function of the generator-level quantities. The vertical lines represent the requirements applied to the reconstruction-level quantities. These efficiencies are calculated using the LM6 MC benchmark, but they do not depend strongly on the underlying physics.

$$f(x) = \frac{\epsilon_\infty}{2} (\text{erf}((x - C)/\sigma) + 1), \quad (4)$$

where ϵ_∞ gives the value of the efficiency plateau at high x , C is the value of x at which the efficiency is equal to 50%, and σ describes how fast the transition is. The values of the fitted parameters are quoted in Table 9.

Table 9: Values of the fitted parameters in Eq. (4) for the E_T^{miss} and H_T selection efficiencies of Fig. 8.

Parameter	$E_T^{\text{miss}} > 150 \text{ GeV}$	$E_T^{\text{miss}} > 200 \text{ GeV}$	$E_T^{\text{miss}} > 275 \text{ GeV}$
ϵ_∞	1.00	1.00	1.00
C	157 GeV	211 GeV	291 GeV
σ	33 GeV	37 GeV	39 GeV
Parameter	$H_T > 125 \text{ GeV}$	$H_T > 300 \text{ GeV}$	$H_T > 600 \text{ GeV}$
ϵ_∞	1.00	1.00	0.99
C	124 GeV	283 GeV	582 GeV
σ	56 GeV	75 GeV	93 GeV

This efficiency model has been validated by comparing the yields from the full reconstruction with the expected yields using generator-level information only and the efficiencies quoted above. In addition to the LM1, LM3, LM6 and LM13 benchmarks considered throughout this paper, we have tested several additional benchmarks (LM2, LM4, LM5, LM7, and LM8) [18]. In general we observe agreement between full reconstruction and the efficiency model within approximately 15%.

9 Summary

We have presented a search for physics beyond the standard model in the opposite-sign dilepton final state using a data sample of proton-proton collisions at a center-of-mass energy of 7 TeV. The data sample corresponds to an integrated luminosity of 4.98 fb^{-1} , and was collected with the CMS detector in 2011. Two complementary search strategies have been performed. The first focuses on models with a specific dilepton production mechanism leading to a characteristic kinematic edge in the dilepton mass distribution, and the second focuses on dilepton events accompanied by large missing transverse energy and significant hadronic activity. This work is motivated by many models of BSM physics, such as supersymmetric models or models with universal extra dimensions. In the absence of evidence for BSM physics, we set upper limits on the BSM contributions to yields in the signal regions. Additional information has been provided to allow testing whether specific models of new physics are excluded by these results. The presented result is the most stringent limit to date from the opposite-sign dilepton final state accompanied by large missing transverse energy and hadronic activity.

Acknowledgements

We congratulate our colleagues in the CERN accelerator departments for the excellent performance of the LHC machine. We thank the technical and administrative staff at CERN and other CMS institutes, and acknowledge support from: FMSR (Austria); FNRS and FWO (Belgium); CNPq, CAPES, FAPERJ, and FAPESP (Brazil); MES (Bulgaria); CERN; CAS, MoST, and NSFC

(China); COLCIENCIAS (Colombia); MSES (Croatia); RPF (Cyprus); MoER, SF0690030s09 and ERDF (Estonia); Academy of Finland, MEC, and HIP (Finland); CEA and CNRS/IN2P3 (France); BMBF, DFG, and HGF (Germany); GSRT (Greece); OTKA and NKTH (Hungary); DAE and DST (India); IPM (Iran); SFI (Ireland); INFN (Italy); NRF and WCU (Korea); LAS (Lithuania); CINVESTAV, CONACYT, SEP, and UASLP-FAI (Mexico); MSI (New Zealand); PAEC (Pakistan); MSHE and NSC (Poland); FCT (Portugal); JINR (Armenia, Belarus, Georgia, Ukraine, Uzbekistan); MON, RosAtom, RAS and RFBR (Russia); MSTD (Serbia); MICINN and CPAN (Spain); Swiss Funding Agencies (Switzerland); NSC (Taipei); TUBITAK and TAEK (Turkey); STFC (United Kingdom); DOE and NSF (USA). Individuals have received support from the Marie-Curie programme and the European Research Council (European Union); the Leventis Foundation; the A. P. Sloan Foundation; the Alexander von Humboldt Foundation; the Belgian Federal Science Policy Office; the Fonds pour la Formation à la Recherche dans l'Industrie et dans l'Agriculture (FRIA-Belgium); the Agentschap voor Innovatie door Wetenschap en Technologie (IWT-Belgium); the Council of Science and Industrial Research, India; and the HOMING PLUS programme of Foundation for Polish Science, cofinanced from European Union, Regional Development Fund.

References

- [1] CMS Collaboration, "The CMS experiment at the CERN LHC", *JINST* **3** (2008) S08004, doi:10.1088/1748-0221/3/08/S08004.
- [2] CMS Collaboration, "Search for physics beyond the standard model in opposite-sign dilepton events at $\sqrt{s} = 7$ TeV", *JHEP* **06** (2011) 026, doi:10.1007/JHEP06(2011)026, arXiv:1103.1348.
- [3] J. Ellis et al., "Exploration of the MSSM with nonuniversal Higgs masses", *Nucl. Phys. B* **652** (2003) 259, doi:10.1016/S0550-3213(02)01144-6, arXiv:hep-ph/0210205.
- [4] J. Ellis et al., "Supersymmetric dark matter in light of WMAP", *Phys. Lett. B* **565** (2003) 176, doi:10.1016/S0370-2693(03)00765-2, arXiv:hep-ph/0303043.
- [5] D. Auto et al., "Yukawa coupling unification in supersymmetric models", *JHEP* **06** (2003) 023, doi:10.1088/1126-6708/2003/06/023, arXiv:hep-ph/0302155.
- [6] A. Bottin et al., "Lower bound on the neutralino mass from new data on CMB and implications for relic neutralinos", *Phys. Rev. D* **68** (2003) 043506, doi:10.1103/PhysRevD.68.043506, arXiv:hep-ph/0304080.
- [7] S. P. Martin, "A Supersymmetry primer", arXiv:hep-ph/9709356.
- [8] J. Wess and B. Zumino, "Supergauge Transformations in Four-Dimensions", *Nucl. Phys. B* **70** (1974) 39, doi:10.1016/0550-3213(74)90355-1.
- [9] M. Battaglia et al., "Contrasting supersymmetry and universal extra dimensions at colliders", (2005). arXiv:hep-ph/0507284.
- [10] V. Khachatryan et al., "Search for supersymmetry in pp collisions at 7 TeV in events with jets and missing transverse energy", *Phys. Lett. B* **698** (2011) 196, doi:10.1016/j.physletb.2011.03.021, arXiv:1101.1628.

- [11] CMS Collaboration, “Search for new physics with same-sign isolated dilepton events with jets and missing transverse energy at the LHC”, *JHEP* **06** (2011) 077, doi:10.1007/JHEP06(2011)077, arXiv:1104.3168.
- [12] ATLAS Collaboration, “Searches for supersymmetry with the ATLAS detector using final states with two leptons and missing transverse momentum in $\sqrt{s} = 7$ TeV proton-proton collisions”, *Phys. Lett. B* **709** (2012) 137, doi:10.1016/j.physletb.2012.01.076, arXiv:1110.6189.
- [13] ATLAS Collaboration, “Search for events with large missing transverse momentum, jets, and at least two tau leptons in 7 TeV proton-proton collision data with the ATLAS detector”, *Phys. Lett. B* **714** (2012) 180, doi:10.1016/j.physletb.2012.06.055, arXiv:1203.6580.
- [14] CMS Collaboration, “First measurement of the cross section for top-quark pair production in proton-proton collisions at $\sqrt{s} = 7$ TeV”, *Phys. Lett. B* **695** (2011) 424, doi:10.1016/j.physletb.2010.11.058, arXiv:1010.5994.
- [15] I. Hinchliffe et al., “Precision SUSY measurements at CERN LHC”, *Phys. Rev. D* **55** (1997) 5520, doi:10.1103/PhysRevD.55.5520.
- [16] G. L. Kane et al., “Study of constrained minimal supersymmetry”, *Phys. Rev. D* **49** (1994) 6173, doi:10.1103/PhysRevD.49.6173, arXiv:hep-ph/9312272.
- [17] A. H. Chamseddine, R. L. Arnowitt, and P. Nath, “Locally Supersymmetric Grand Unification”, *Phys. Rev. Lett.* **49** (1982) 970, doi:10.1103/PhysRevLett.49.970.
- [18] CMS Collaboration, “CMS technical design report, volume II: Physics performance”, *J. Phys. G* **34** (2007) 995, doi:10.1088/0954-3899/34/6/S01.
- [19] CMS Collaboration, “Commissioning of the Particle-Flow Reconstruction in Minimum-Bias and Jet Events from pp Collisions at 7 TeV”, CMS Physics Analysis Summary CMS-PAS-PFT-10-002, (2010).
- [20] T. Sjöstrand, S. Mrenna, and P. Z. Skands, “PYTHIA 6.4 physics and manual”, *JHEP* **05** (2006) 026, doi:10.1088/1126-6708/2006/05/026, arXiv:hep-ph/0603175.
- [21] J. Alwall, “MadGraph/MadEvent v4: the new web generation”, *JHEP* **09** (2007) 028, doi:10.1088/1126-6708/2007/09/028.
- [22] S. Frixione, P. Nason, and C. Oleari, “Matching NLO QCD computations with parton shower simulations: the POWHEG method”, *JHEP* **11** (2007) 070, doi:10.1088/1126-6708/2007/11/070, arXiv:0709.2092.
- [23] P. M. Nadolsky et al., “Implications of CTEQ global analysis for collider observables”, *Phys. Rev. D* **78** (2008) 013004, doi:10.1103/PhysRevD.78.013004, arXiv:0802.0007.
- [24] CMS Collaboration, “Measurement of the Underlying Event Activity at the LHC with $\sqrt{s} = 7$ TeV and Comparison with $\sqrt{s} = 0.9$ TeV”, *JHEP* **1109** (2011) 109, doi:10.1007/JHEP09(2011)109, arXiv:1107.0330.
- [25] GEANT4 Collaboration, “GEANT4—a simulation toolkit”, *Nucl. Instrum. Meth. A* **506** (2003) 250, doi:10.1016/S0168-9002(03)01368-8.

- [26] CMS Collaboration, "CMS Tracking Performance Results from early LHC Operation", *Eur. Phys. J. C* **70** (2010) 1165, doi:10.1140/epjc/s10052-010-1491-3, arXiv:1007.1988.
- [27] CMS Collaboration, "Performance of tau reconstruction algorithms in 2010 data collected with CMS", CMS Physics Analysis Summary CMS-PAS-TAU-11-001, (2011).
- [28] M. Cacciari, G. P. Salam, and G. Soyez, "The anti- k_t jet clustering algorithm", *JHEP* **04** (2008) 063, doi:10.1088/1126-6708/2008/04/063, arXiv:0802.1189.
- [29] CMS Collaboration, "First Measurement of the Cross Section for Top-Quark Pair Production in Proton-Proton Collisions at $\sqrt{s} = 7$ TeV", *Phys. Lett. B* **695** (2011) 424, doi:10.1016/j.physletb.2010.11.058, arXiv:1010.5994.
- [30] CMS Collaboration, "Measurement of the $t\bar{t}$ production cross section and the top quark mass in the dilepton channel in pp collisions at $\sqrt{s} = 7$ TeV", *JHEP* **07** (2011) 049, doi:10.1007/JHEP07(2011)049, arXiv:1105.5661.
- [31] CMS Collaboration, "Measurement of the $t\bar{t}$ production cross section in pp collisions at 7 TeV in lepton+jets events using b -quark jet identification", *Phys. Rev. D* **84** (2011) 092004, doi:10.1103/PhysRevD.84.092004, arXiv:1108.3773.
- [32] E. Gross and O. Vitells, "Trial factors for the look elsewhere effect in high energy physics", *Eur. Phys. J. C* **70** (2010) 525, doi:10.1140/epjc/s10052-010-1470-8, arXiv:1005.1891.
- [33] V. Pavlunin, "Modeling missing transverse energy in V+jets at CERN LHC", *Phys. Rev. D* **81** (2010) 035005, doi:10.1103/PhysRevD.81.035005, arXiv:0906.5016.
- [34] J. A. Aguilar-Saavedra et al., "Probing anomalous Wtb couplings in top pair decays", *Eur. Phys. J. C* **50** (2007) 519, doi:10.1140/epjc/s10052-007-0289-4, arXiv:hep-ph/0605190.
- [35] A. Czarnecki, J. G. Korner, and J. H. Piclum, "Helicity fractions of W bosons from top quark decays at NNLO in QCD", *Phys. Rev. D* **81** (2010) 111503, doi:10.1103/PhysRevD.81.111503, arXiv:1005.2625.
- [36] CDF Collaboration, "Measurement of W-Boson Polarization in Top-quark Decay in $p\bar{p}$ Collisions at $\sqrt{s} = 1.96$ TeV", *Phys. Rev. Lett.* **105** (2010) 042002, doi:10.1103/PhysRevLett.105.042002, arXiv:1003.0224.
- [37] CMS Collaboration, "Search for neutral Higgs bosons decaying to tau pairs in pp collisions at $\sqrt{s} = 7$ TeV", *Phys. Lett. B* (2012) 68, doi:10.1016/j.physletb.2012.05.028, arXiv:1202.4083.
- [38] CMS Collaboration, "Determination of Jet Energy Calibration and Transverse Momentum Resolution in CMS", *JINST* **6** (2011) P11002, doi:10.1088/1748-0221/6/11/P11002, arXiv:1107.4277.
- [39] Particle Data Group Collaboration, "Review of particle physics", *Phys. G* **37** (2010) 075021, doi:10.1088/0954-3899/37/7A/075021.
- [40] B. C. Allanach, "SOFTSUSY: a program for calculating supersymmetric spectra", *Comput. Phys. Commun.* **143** (2002) 305, doi:10.1016/S0010-4655(01)00460-X.

-
- [41] W. Beenakker et al., “Squark and Gluino Production at Hadron Colliders”, *Nucl. Phys. B* **492** (1997) 51, doi:10.1016/S0550-3213(97)00084-9.
- [42] M. Botje et al., “The PDF4LHC Working Group Interim Recommendations”, (2011).
arXiv:1101.0538.
- [43] LEPSUSYWG, ALEPH, DELPHI, L3 and OPAL experiments, “LSP mass limit in Minimal SUGRA”,. LEPSUSYWG/02-06.2.

A The CMS Collaboration

Yerevan Physics Institute, Yerevan, Armenia

S. Chatrchyan, V. Khachatryan, A.M. Sirunyan, A. Tumasyan

Institut für Hochenergiephysik der OeAW, Wien, Austria

W. Adam, T. Bergauer, M. Dragicevic, J. Erö, C. Fabjan, M. Friedl, R. Frühwirth, V.M. Ghete, J. Hammer, N. Hörmann, J. Hrubec, M. Jeitler, W. Kiesenhofer, V. Knünz, M. Krammer, D. Liko, I. Mikulec, M. Pernicka[†], B. Rahbaran, C. Rohringer, H. Rohringer, R. Schöfbeck, J. Strauss, A. Taurok, P. Wagner, W. Waltenberger, G. Walzel, E. Widl, C.-E. Wulz

National Centre for Particle and High Energy Physics, Minsk, Belarus

V. Mossolov, N. Shumeiko, J. Suarez Gonzalez

Universiteit Antwerpen, Antwerpen, Belgium

S. Bansal, T. Cornelis, E.A. De Wolf, X. Janssen, S. Luyckx, T. Maes, L. Mucibello, S. Ochesanu, B. Roland, R. Rougny, M. Selvaggi, Z. Staykova, H. Van Haevermaet, P. Van Mechelen, N. Van Remortel, A. Van Spilbeeck

Vrije Universiteit Brussel, Brussel, Belgium

F. Blekman, S. Blyweert, J. D'Hondt, R. Gonzalez Suarez, A. Kalogeropoulos, M. Maes, A. Olbrechts, W. Van Doninck, P. Van Mulders, G.P. Van Onsem, I. Villella

Université Libre de Bruxelles, Bruxelles, Belgium

O. Charaf, B. Clerbaux, G. De Lentdecker, V. Dero, A.P.R. Gay, T. Hreus, A. Léonard, P.E. Marage, T. Reis, L. Thomas, C. Vander Velde, P. Vanlaer, J. Wang

Ghent University, Ghent, Belgium

V. Adler, K. Bernaert, A. Cimmino, S. Costantini, G. Garcia, M. Grunewald, B. Klein, J. Lellouch, A. Marinov, J. McCartin, A.A. Ocampo Rios, D. Ryckbosch, N. Strobbe, F. Thyssen, M. Tytgat, L. Vanelderen, P. Verwilligen, S. Walsh, E. Yazgan, N. Zaganidis

Université Catholique de Louvain, Louvain-la-Neuve, Belgium

S. Basegmez, G. Bruno, R. Castello, A. Caudron, L. Ceard, C. Delaere, T. du Pree, D. Favart, L. Forthomme, A. Giammanco¹, J. Hollar, V. Lemaître, J. Liao, O. Militaru, C. Nuttens, D. Pagano, L. Perrini, A. Pin, K. Piotrkowski, N. Schul, J.M. Vizan Garcia

Université de Mons, Mons, Belgium

N. Belyi, T. Caebergs, E. Daubie, G.H. Hammad

Centro Brasileiro de Pesquisas Fisicas, Rio de Janeiro, Brazil

G.A. Alves, M. Correa Martins Junior, D. De Jesus Damiao, T. Martins, M.E. Pol, M.H.G. Souza

Universidade do Estado do Rio de Janeiro, Rio de Janeiro, Brazil

W.L. Aldá Júnior, W. Carvalho, A. Custódio, E.M. Da Costa, C. De Oliveira Martins, S. Fonseca De Souza, D. Matos Figueiredo, L. Mundim, H. Nogima, V. Oguri, W.L. Prado Da Silva, A. Santoro, L. Soares Jorge, A. Sznajder

Instituto de Fisica Teorica, Universidade Estadual Paulista, Sao Paulo, Brazil

C.A. Bernardes², F.A. Dias³, T.R. Fernandez Perez Tomei, E. M. Gregores², C. Lagana, F. Marinho, P.G. Mercadante², S.F. Novaes, Sandra S. Padula

Institute for Nuclear Research and Nuclear Energy, Sofia, Bulgaria

V. Genchev⁴, P. Iaydjiev⁴, S. Piperov, M. Rodozov, S. Stoykova, G. Sultanov, V. Tcholakov, R. Trayanov, M. Vutova

University of Sofia, Sofia, Bulgaria

A. Dimitrov, R. Hadjiiska, V. Kozhuharov, L. Litov, B. Pavlov, P. Petkov

Institute of High Energy Physics, Beijing, China

J.G. Bian, G.M. Chen, H.S. Chen, C.H. Jiang, D. Liang, S. Liang, X. Meng, J. Tao, J. Wang, X. Wang, Z. Wang, H. Xiao, M. Xu, J. Zang, Z. Zhang

State Key Lab. of Nucl. Phys. and Tech., Peking University, Beijing, China

C. Asawatangtrakuldee, Y. Ban, S. Guo, Y. Guo, W. Li, S. Liu, Y. Mao, S.J. Qian, H. Teng, S. Wang, B. Zhu, W. Zou

Universidad de Los Andes, Bogota, Colombia

C. Avila, J.P. Gomez, B. Gomez Moreno, A.F. Osorio Oliveros, J.C. Sanabria

Technical University of Split, Split, Croatia

N. Godinovic, D. Lelas, R. Plestina⁵, D. Polic, I. Puljak⁴

University of Split, Split, Croatia

Z. Antunovic, M. Kovac

Institute Rudjer Boskovic, Zagreb, Croatia

V. Brigljevic, S. Duric, K. Kadija, J. Luetic, S. Morovic

University of Cyprus, Nicosia, Cyprus

A. Attikis, M. Galanti, G. Mavromanolakis, J. Mousa, C. Nicolaou, F. Ptochos, P.A. Razis

Charles University, Prague, Czech Republic

M. Finger, M. Finger Jr.

Academy of Scientific Research and Technology of the Arab Republic of Egypt, Egyptian Network of High Energy Physics, Cairo, Egypt

Y. Assran⁶, S. Elgammal⁷, A. Ellithi Kamel⁸, S. Khalil⁷, M.A. Mahmoud⁹, A. Radi^{10,11}

National Institute of Chemical Physics and Biophysics, Tallinn, Estonia

M. Kadastik, M. Müntel, M. Raidal, L. Rebane, A. Tiko

Department of Physics, University of Helsinki, Helsinki, Finland

V. Azzolini, P. Eerola, G. Fedi, M. Voutilainen

Helsinki Institute of Physics, Helsinki, Finland

J. Härkönen, A. Heikkinen, V. Karimäki, R. Kinnunen, M.J. Kortelainen, T. Lampén, K. Lassila-Perini, S. Lehti, T. Lindén, P. Luukka, T. Mäenpää, T. Peltola, E. Tuominen, J. Tuominiemi, E. Tuovinen, D. Ungaro, L. Wendland

Lappeenranta University of Technology, Lappeenranta, Finland

K. Banzuzi, A. Korpela, T. Tuuva

DSM/IRFU, CEA/Saclay, Gif-sur-Yvette, France

M. Besancon, S. Choudhury, M. DeJardin, D. Denegri, B. Fabbro, J.L. Faure, F. Ferri, S. Ganjour, A. Givernaud, P. Gras, G. Hamel de Monchenault, P. Jarry, E. Locci, J. Malcles, L. Millischer, A. Nayak, J. Rander, A. Rosowsky, I. Shreyber, M. Titov

Laboratoire Leprince-Ringuet, Ecole Polytechnique, IN2P3-CNRS, Palaiseau, France

S. Baffioni, F. Beaudette, L. Benhabib, L. Bianchini, M. Bluj¹², C. Broutin, P. Busson, C. Charlot, N. Daci, T. Dahms, L. Dobrzynski, R. Granier de Cassagnac, M. Haguener, P. Miné, C. Mironov, C. Ochando, P. Paganini, D. Sabes, R. Salerno, Y. Sirois, C. Veelken, A. Zabi

Institut Pluridisciplinaire Hubert Curien, Université de Strasbourg, Université de Haute Alsace Mulhouse, CNRS/IN2P3, Strasbourg, France

J.-L. Agram¹³, J. Andrea, D. Bloch, D. Bodin, J.-M. Brom, M. Cardaci, E.C. Chabert, C. Collard, E. Conte¹³, F. Drouhin¹³, C. Ferro, J.-C. Fontaine¹³, D. Gelé, U. Goerlach, P. Juillot, M. Karim¹³, A.-C. Le Bihan, P. Van Hove

Centre de Calcul de l'Institut National de Physique Nucleaire et de Physique des Particules (IN2P3), Villeurbanne, France

F. Fassi, D. Mercier

Université de Lyon, Université Claude Bernard Lyon 1, CNRS-IN2P3, Institut de Physique Nucléaire de Lyon, Villeurbanne, France

S. Beauceron, N. Beaupere, O. Bondu, G. Boudoul, H. Brun, J. Chasserat, R. Chierici⁴, D. Contardo, P. Depasse, H. El Mamouni, J. Fay, S. Gascon, M. Gouzevitch, B. Ille, T. Kurca, M. Lethuillier, L. Mirabito, S. Perries, V. Sordini, S. Tosi, Y. Tschudi, P. Verdier, S. Viret

Institute of High Energy Physics and Informatization, Tbilisi State University, Tbilisi, Georgia

Z. Tsamalaidze¹⁴

RWTH Aachen University, I. Physikalisches Institut, Aachen, Germany

G. Anagnostou, S. Beranek, M. Edelhoff, L. Feld, N. Heracleous, O. Hindrichs, R. Jussen, K. Klein, J. Merz, A. Ostapchuk, A. Perieanu, F. Raupach, J. Sammet, S. Schael, D. Sprenger, H. Weber, B. Wittmer, V. Zhukov¹⁵

RWTH Aachen University, III. Physikalisches Institut A, Aachen, Germany

M. Ata, J. Caudron, E. Dietz-Laursonn, D. Duchardt, M. Erdmann, R. Fischer, A. Güth, T. Hebbeker, C. Heidemann, K. Hoepfner, D. Klingebiel, P. Kreuzer, J. Lingemann, C. Magass, M. Merschmeyer, A. Meyer, M. Olschewski, P. Papacz, H. Pieta, H. Reithler, S.A. Schmitz, L. Sonnenschein, J. Steggemann, D. Teyssier, M. Weber

RWTH Aachen University, III. Physikalisches Institut B, Aachen, Germany

M. Bontenackels, V. Cherepanov, M. Davids, G. Flügge, H. Geenen, M. Geisler, W. Haj Ahmad, F. Hoehle, B. Kargoll, T. Kress, Y. Kuessel, A. Linn, A. Nowack, L. Perchalla, O. Pooth, J. Rennefeld, P. Sauerland, A. Stahl

Deutsches Elektronen-Synchrotron, Hamburg, Germany

M. Aldaya Martin, J. Behr, W. Behrenhoff, U. Behrens, M. Bergholz¹⁶, A. Bethani, K. Borras, A. Burgmeier, A. Cakir, L. Calligaris, A. Campbell, E. Castro, F. Costanza, D. Dammann, G. Eckerlin, D. Eckstein, G. Flucke, A. Geiser, I. Glushkov, P. Gunnellini, S. Habib, J. Hauk, G. Hellwig, H. Jung⁴, M. Kasemann, P. Katsas, C. Kleinwort, H. Kluge, A. Knutsson, M. Krämer, D. Krücker, E. Kuznetsova, W. Lange, W. Lohmann¹⁶, B. Lutz, R. Mankel, I. Marfin, M. Marienfeld, I.-A. Melzer-Pellmann, A.B. Meyer, J. Mnich, A. Mussgiller, S. Naumann-Emme, J. Olzem, H. Perrey, A. Petrukhin, D. Pitzl, A. Raspereza, P.M. Ribeiro Cipriano, C. Riedl, M. Rosin, J. Salfeld-Nebgen, R. Schmidt¹⁶, T. Schoerner-Sadenius, N. Sen, A. Spiridonov, M. Stein, R. Walsh, C. Wissing

University of Hamburg, Hamburg, Germany

C. Autermann, V. Blobel, S. Bobrovskiy, J. Draeger, H. Enderle, J. Erfle, U. Gebbert, M. Görner, T. Hermanns, R.S. Höing, K. Kaschube, G. Kaussen, H. Kirschenmann, R. Klanner, J. Lange, B. Mura, F. Nowak, T. Peiffer, N. Pietsch, D. Rathjens, C. Sander, H. Schettler, P. Schleper, E. Schlieckau, A. Schmidt, M. Schröder, T. Schum, M. Seidel, H. Stadie, G. Steinbrück, J. Thomsen

Institut für Experimentelle Kernphysik, Karlsruhe, Germany

C. Barth, J. Berger, C. Böser, T. Chwalek, W. De Boer, A. Descroix, A. Dierlamm, M. Feindt, M. Guthoff⁴, C. Hackstein, F. Hartmann, T. Hauth⁴, M. Heinrich, H. Held, K.H. Hoffmann, S. Honc, I. Katkov¹⁵, J.R. Komaragiri, D. Martschei, S. Mueller, Th. Müller, M. Niegel, A. Nürnberg, O. Oberst, A. Oehler, J. Ott, G. Quast, K. Rabbertz, F. Ratnikov, N. Ratnikova, S. Röcker, A. Scheurer, F.-P. Schilling, G. Schott, H.J. Simonis, F.M. Stober, D. Troendle, R. Ulrich, J. Wagner-Kuhr, S. Wayand, T. Weiler, M. Zeise

Institute of Nuclear Physics "Demokritos", Aghia Paraskevi, Greece

G. Daskalakis, T. Gerasis, S. Kesisoglou, A. Kyriakis, D. Loukas, I. Manolakos, A. Markou, C. Markou, C. Mavrommatis, E. Ntomari

University of Athens, Athens, Greece

L. Gouskos, T.J. Mertzimekis, A. Panagiotou, N. Saoulidou

University of Ioánnina, Ioánnina, Greece

I. Evangelou, C. Foudas⁴, P. Kokkas, N. Manthos, I. Papadopoulos, V. Patras

KFKI Research Institute for Particle and Nuclear Physics, Budapest, Hungary

G. Bencze, C. Hajdu⁴, P. Hidas, D. Horvath¹⁷, K. Krajczar¹⁸, B. Radics, F. Sikler⁴, V. Veszpremi, G. Vesztergombi¹⁸

Institute of Nuclear Research ATOMKI, Debrecen, Hungary

N. Beni, S. Czellar, J. Molnar, J. Palinkas, Z. Szillasi

University of Debrecen, Debrecen, Hungary

J. Karancsi, P. Raics, Z.L. Trocsanyi, B. Ujvari

Panjab University, Chandigarh, India

S.B. Beri, V. Bhatnagar, N. Dhingra, R. Gupta, M. Jindal, M. Kaur, J.M. Kohli, M.Z. Mehta, N. Nishu, L.K. Saini, A. Sharma, J. Singh

University of Delhi, Delhi, India

Ashok Kumar, Arun Kumar, S. Ahuja, A. Bhardwaj, B.C. Choudhary, S. Malhotra, M. Naimuddin, K. Ranjan, V. Sharma, R.K. Shivpuri

Saha Institute of Nuclear Physics, Kolkata, India

S. Banerjee, S. Bhattacharya, S. Dutta, B. Gomber, Sa. Jain, Sh. Jain, R. Khurana, S. Sarkar, M. Sharan

Bhabha Atomic Research Centre, Mumbai, India

A. Abdulsalam, R.K. Choudhury, D. Dutta, S. Kailas, V. Kumar, P. Mehta, A.K. Mohanty⁴, L.M. Pant, P. Shukla

Tata Institute of Fundamental Research - EHEP, Mumbai, India

T. Aziz, S. Ganguly, M. Guchait¹⁹, M. Maity²⁰, G. Majumder, K. Mazumdar, G.B. Mohanty, B. Parida, K. Sudhakar, N. Wickramage

Tata Institute of Fundamental Research - HECR, Mumbai, India

S. Banerjee, S. Dugad

Institute for Research in Fundamental Sciences (IPM), Tehran, Iran

H. Arfaei, H. Bakhshiansohi²¹, S.M. Etesami²², A. Fahim²¹, M. Hashemi, H. Hesari, A. Jafari²¹, M. Khakzad, A. Mohammadi²³, M. Mohammadi Najafabadi, S. Paktinat Mehdiabadi, B. Safarzadeh²⁴, M. Zeinali²²

INFN Sezione di Bari ^a, Università di Bari ^b, Politecnico di Bari ^c, Bari, Italy

M. Abbrescia^{a,b}, L. Barbone^{a,b}, C. Calabria^{a,b,4}, S.S. Chhibra^{a,b}, A. Colaleo^a, D. Creanza^{a,c}, N. De Filippis^{a,c,4}, M. De Palma^{a,b}, L. Fiore^a, G. Iaselli^{a,c}, L. Lusito^{a,b}, G. Maggi^{a,c}, M. Maggi^a, B. Marangelli^{a,b}, S. My^{a,c}, S. Nuzzo^{a,b}, N. Pacifico^{a,b}, A. Pompili^{a,b}, G. Pugliese^{a,c}, G. Selvaggi^{a,b}, L. Silvestris^a, G. Singh^{a,b}, R. Venditti, G. Zito^a

INFN Sezione di Bologna ^a, Università di Bologna ^b, Bologna, Italy

G. Abbiendi^a, A.C. Benvenuti^a, D. Bonacorsi^{a,b}, S. Braibant-Giacomelli^{a,b}, L. Brigliadori^{a,b}, P. Capiluppi^{a,b}, A. Castro^{a,b}, F.R. Cavallo^a, M. Cuffiani^{a,b}, G.M. Dallavalle^a, F. Fabbri^a, A. Fanfani^{a,b}, D. Fasanella^{a,b,4}, P. Giacomelli^a, C. Grandi^a, L. Guiducci, S. Marcellini^a, G. Masetti^a, M. Meneghelli^{a,b,4}, A. Montanari^a, F.L. Navarria^{a,b}, F. Odorici^a, A. Perrotta^a, F. Primavera^{a,b}, A.M. Rossi^{a,b}, T. Rovelli^{a,b}, G. Siroli^{a,b}, R. Travaglini^{a,b}

INFN Sezione di Catania ^a, Università di Catania ^b, Catania, Italy

S. Albergo^{a,b}, G. Cappello^{a,b}, M. Chiorboli^{a,b}, S. Costa^{a,b}, R. Potenza^{a,b}, A. Tricomi^{a,b}, C. Tuve^{a,b}

INFN Sezione di Firenze ^a, Università di Firenze ^b, Firenze, Italy

G. Barbagli^a, V. Ciulli^{a,b}, C. Civinini^a, R. D'Alessandro^{a,b}, E. Focardi^{a,b}, S. Frosali^{a,b}, E. Gallo^a, S. Gonzi^{a,b}, M. Meschini^a, S. Paoletti^a, G. Sguazzoni^a, A. Tropiano^{a,4}

INFN Laboratori Nazionali di Frascati, Frascati, Italy

L. Benussi, S. Bianco, S. Colafranceschi²⁵, F. Fabbri, D. Piccolo

INFN Sezione di Genova, Genova, Italy

P. Fabbriatore, R. Musenich

INFN Sezione di Milano-Bicocca ^a, Università di Milano-Bicocca ^b, Milano, Italy

A. Benaglia^{a,b,4}, F. De Guio^{a,b}, L. Di Matteo^{a,b,4}, S. Fiorendi^{a,b}, S. Gennai^{a,4}, A. Ghezzi^{a,b}, S. Malvezzi^a, R.A. Manzoni^{a,b}, A. Martelli^{a,b}, A. Massironi^{a,b,4}, D. Menasce^a, L. Moroni^a, M. Paganoni^{a,b}, D. Pedrini^a, S. Ragazzi^{a,b}, N. Redaelli^a, S. Sala^a, T. Tabarelli de Fatis^{a,b}

INFN Sezione di Napoli ^a, Università di Napoli "Federico II" ^b, Napoli, Italy

S. Buontempo^a, C.A. Carrillo Montoya^{a,4}, N. Cavallo^{a,26}, A. De Cosa^{a,b,4}, O. Dogangun^{a,b}, F. Fabozzi^{a,26}, A.O.M. Iorio^{a,4}, L. Lista^a, S. Meola^{a,27}, M. Merola^{a,b}, P. Paolucci^{a,4}

INFN Sezione di Padova ^a, Università di Padova ^b, Università di Trento (Trento) ^c, Padova, Italy

P. Azzi^a, N. Bacchetta^{a,4}, P. Bellan^{a,b}, A. Branca^{a,4}, R. Carlin^{a,b}, P. Checchia^a, T. Dorigo^a, F. Gasparini^{a,b}, U. Gasparini^{a,b}, A. Gozzelino^a, K. Kanishchev^{a,c}, S. Lacaprara^a, I. Lazzizzera^{a,c}, M. Margoni^{a,b}, A.T. Meneguzzo^{a,b}, M. Nespolo^{a,4}, J. Pazzini^a, L. Perrozzi^a, N. Pozzobon^{a,b}, P. Ronchese^{a,b}, F. Simonetto^{a,b}, E. Torassa^a, M. Tosi^{a,b,4}, S. Vanini^{a,b}, P. Zotto^{a,b}, A. Zucchetta^a, G. Zumerle^{a,b}

INFN Sezione di Pavia ^a, Università di Pavia ^b, Pavia, Italy

M. Gabusi^{a,b}, S.P. Ratti^{a,b}, C. Riccardi^{a,b}, P. Torre^{a,b}, P. Vitulo^{a,b}

INFN Sezione di Perugia ^a, Università di Perugia ^b, Perugia, Italy

M. Biasini^{a,b}, G.M. Bilei^a, L. Fanò^{a,b}, P. Lariccia^{a,b}, A. Lucaroni^{a,b,4}, G. Mantovani^{a,b}, M. Menichelli^a, A. Nappi^{a,b}, F. Romeo^{a,b}, A. Saha, A. Santocchia^{a,b}, S. Taroni^{a,b,4}

INFN Sezione di Pisa ^a, Università di Pisa ^b, Scuola Normale Superiore di Pisa ^c, Pisa, Italy

P. Azzurri^{a,c}, G. Bagliesi^a, T. Boccali^a, G. Broccolo^{a,c}, R. Castaldi^a, R.T. D'Agnolo^{a,c}, R. Dell'Orso^a, F. Fiori^{a,b,4}, L. Foà^{a,c}, A. Giassi^a, A. Kraan^a, F. Ligabue^{a,c}, T. Lomtadze^a, L. Martini^{a,28}, A. Messineo^{a,b}, F. Palla^a, F. Palmonari^a, A. Rizzi^{a,b}, A.T. Serban^{a,29}, P. Spagnolo^a, P. Squillacioti^{a,4}, R. Tenchini^a, G. Tonelli^{a,b,4}, A. Venturi^{a,4}, P.G. Verdini^a

INFN Sezione di Roma ^a, Università di Roma "La Sapienza" ^b, Roma, Italy

L. Barone^{a,b}, F. Cavallari^a, D. Del Re^{a,b,4}, M. Diemoz^a, M. Grassi^{a,b,4}, E. Longo^{a,b}, P. Meridiani^{a,4}, F. Micheli^{a,b}, S. Nourbakhsh^{a,b}, G. Organtini^{a,b}, R. Paramatti^a, S. Rahatlou^{a,b}, M. Sigamani^a, L. Soffi^{a,b}

INFN Sezione di Torino ^a, Università di Torino ^b, Università del Piemonte Orientale (Novara) ^c, Torino, Italy

N. Amapane^{a,b}, R. Arcidiacono^{a,c}, S. Argiro^{a,b}, M. Arneodo^{a,c}, C. Biino^a, C. Botta^{a,b}, N. Cartiglia^a, M. Costa^{a,b}, N. Demaria^a, A. Graziano^{a,b}, C. Mariotti^{a,4}, S. Maselli^a, E. Migliore^{a,b}, V. Monaco^{a,b}, M. Musich^{a,4}, M.M. Obertino^{a,c}, N. Pastrone^a, M. Pelliccioni^a, A. Potenza^{a,b}, A. Romero^{a,b}, M. Ruspa^{a,c}, R. Sacchi^{a,b}, V. Sola^{a,b}, A. Solano^{a,b}, A. Staiano^a, A. Vilela Pereira^a

INFN Sezione di Trieste ^a, Università di Trieste ^b, Trieste, Italy

S. Belforte^a, F. Cossutti^a, G. Della Ricca^{a,b}, B. Gobbo^a, M. Marone^{a,b,4}, D. Montanino^{a,b,4}, A. Penzo^a, A. Schizzi^{a,b}

Kangwon National University, Chunchon, Korea

S.G. Heo, T.Y. Kim, S.K. Nam

Kyungpook National University, Daegu, Korea

S. Chang, J. Chung, D.H. Kim, G.N. Kim, D.J. Kong, H. Park, S.R. Ro, D.C. Son, T. Son

Chonnam National University, Institute for Universe and Elementary Particles, Kwangju, Korea

J.Y. Kim, Zero J. Kim, S. Song

Konkuk University, Seoul, Korea

H.Y. Jo

Korea University, Seoul, Korea

S. Choi, D. Gyun, B. Hong, M. Jo, H. Kim, T.J. Kim, K.S. Lee, D.H. Moon, S.K. Park, E. Seo

University of Seoul, Seoul, Korea

M. Choi, S. Kang, H. Kim, J.H. Kim, C. Park, I.C. Park, S. Park, G. Ryu

Sungkyunkwan University, Suwon, Korea

Y. Cho, Y. Choi, Y.K. Choi, J. Goh, M.S. Kim, E. Kwon, B. Lee, J. Lee, S. Lee, H. Seo, I. Yu

Vilnius University, Vilnius, Lithuania

M.J. Bilinskas, I. Grigelionis, M. Janulis, A. Juodagalvis

Centro de Investigacion y de Estudios Avanzados del IPN, Mexico City, Mexico

H. Castilla-Valdez, E. De La Cruz-Burelo, I. Heredia-de La Cruz, R. Lopez-Fernandez, R. Magaña Villalba, J. Martínez-Ortega, A. Sánchez-Hernández, L.M. Villasenor-Cendejas

Universidad Iberoamericana, Mexico City, Mexico

S. Carrillo Moreno, F. Vazquez Valencia

Benemerita Universidad Autonoma de Puebla, Puebla, Mexico

H.A. Salazar Ibarguen

Universidad Autónoma de San Luis Potosí, San Luis Potosí, Mexico

E. Casimiro Linares, A. Morelos Pineda, M.A. Reyes-Santos

University of Auckland, Auckland, New Zealand

D. Krofcheck

University of Canterbury, Christchurch, New Zealand

A.J. Bell, P.H. Butler, R. Doesburg, S. Reucroft, H. Silverwood

National Centre for Physics, Quaid-I-Azam University, Islamabad, Pakistan

M. Ahmad, M.I. Asghar, H.R. Hoorani, S. Khalid, W.A. Khan, T. Khurshid, S. Qazi, M.A. Shah, M. Shoaib

Institute of Experimental Physics, Faculty of Physics, University of Warsaw, Warsaw, Poland

G. Brona, K. Bunkowski, M. Cwiok, W. Dominik, K. Doroba, A. Kalinowski, M. Konecki, J. Krolikowski

Soltan Institute for Nuclear Studies, Warsaw, Poland

H. Bialkowska, B. Boimska, T. Frueboes, R. Gokieli, M. Górski, M. Kazana, K. Nawrocki, K. Romanowska-Rybinska, M. Szleper, G. Wrochna, P. Zalewski

Laboratório de Instrumentação e Física Experimental de Partículas, Lisboa, Portugal

N. Almeida, P. Bargassa, A. David, P. Faccioli, M. Fernandes, P.G. Ferreira Parracho, M. Gallinaro, J. Seixas, J. Varela, P. Vischia

Joint Institute for Nuclear Research, Dubna, Russia

I. Belotelov, P. Bunin, M. Gavrilenko, I. Golutvin, I. Gorbunov, A. Kamenev, V. Karjavin, G. Kozlov, A. Lanev, A. Malakhov, P. Moisezenz, V. Palichik, V. Perelygin, S. Shmatov, V. Smirnov, A. Volodko, A. Zarubin

Petersburg Nuclear Physics Institute, Gatchina (St Petersburg), Russia

S. Evstyukhin, V. Golovtsov, Y. Ivanov, V. Kim, P. Levchenko, V. Murzin, V. Oreshkin, I. Smirnov, V. Sulimov, L. Uvarov, S. Vavilov, A. Vorobyev, An. Vorobyev

Institute for Nuclear Research, Moscow, Russia

Yu. Andreev, A. Dermenev, S. Gninenko, N. Golubev, M. Kirsanov, N. Krasnikov, V. Matveev, A. Pashenkov, D. Tlisov, A. Toropin

Institute for Theoretical and Experimental Physics, Moscow, Russia

V. Epshteyn, M. Erofeeva, V. Gavrilov, M. Kossov⁴, N. Lychkovskaya, V. Popov, G. Safronov, S. Semenov, V. Stolin, E. Vlasov, A. Zhokin

Moscow State University, Moscow, Russia

A. Belyaev, E. Boos, M. Dubinin³, L. Dudko, A. Ershov, A. Gribushin, V. Klyukhin, O. Kodolova, I. Lokhtin, A. Markina, S. Obraztsov, M. Perfilov, S. Petrushanko, A. Popov, L. Sarycheva[†], V. Savrin, A. Snigirev

P.N. Lebedev Physical Institute, Moscow, Russia

V. Andreev, M. Azarkin, I. Dremin, M. Kirakosyan, A. Leonidov, G. Mesyats, S.V. Rusakov, A. Vinogradov

State Research Center of Russian Federation, Institute for High Energy Physics, Protvino, Russia

I. Azhgirey, I. Bayshev, S. Bitioukov, V. Grishin⁴, V. Kachanov, D. Konstantinov, A. Korablev, V. Krychkin, V. Petrov, R. Ryutin, A. Sobol, L. Tourtchanovitch, S. Troshin, N. Tyurin, A. Uzunian, A. Volkov

University of Belgrade, Faculty of Physics and Vinca Institute of Nuclear Sciences, Belgrade, Serbia

P. Adzic³⁰, M. Djordjevic, M. Ekmedzic, D. Krpic³⁰, J. Milosevic

Centro de Investigaciones Energéticas Medioambientales y Tecnológicas (CIEMAT), Madrid, Spain

M. Aguilar-Benitez, J. Alcaraz Maestre, P. Arce, C. Battilana, E. Calvo, M. Cerrada, M. Chamizo Llatas, N. Colino, B. De La Cruz, A. Delgado Peris, C. Diez Pardos, D. Domínguez Vázquez, C. Fernandez Bedoya, J.P. Fernández Ramos, A. Ferrando, J. Flix, M.C. Fouz, P. Garcia-Abia, O. Gonzalez Lopez, S. Goy Lopez, J.M. Hernandez, M.I. Josa, G. Merino, J. Puerta Pelayo, A. Quintario Olmeda, I. Redondo, L. Romero, J. Santaolalla, M.S. Soares, C. Willmott

Universidad Autónoma de Madrid, Madrid, Spain

C. Albajar, G. Codispoti, J.F. de Trocóniz

Universidad de Oviedo, Oviedo, Spain

J. Cuevas, J. Fernandez Menendez, S. Folgueras, I. Gonzalez Caballero, L. Lloret Iglesias, J. Piedra Gomez³¹

Instituto de Física de Cantabria (IFCA), CSIC-Universidad de Cantabria, Santander, Spain

J.A. Brochero Cifuentes, I.J. Cabrillo, A. Calderon, S.H. Chuang, J. Duarte Campderros, M. Felcini³², M. Fernandez, G. Gomez, J. Gonzalez Sanchez, C. Jorda, P. Lobelle Pardo, A. Lopez Virto, J. Marco, R. Marco, C. Martinez Rivero, F. Matorras, F.J. Munoz Sanchez, T. Rodrigo, A.Y. Rodríguez-Marrero, A. Ruiz-Jimeno, L. Scodellaro, M. Sobron Sanudo, I. Vila, R. Vilar Cortabitarte

CERN, European Organization for Nuclear Research, Geneva, Switzerland

D. Abbaneo, E. Auffray, G. Auzinger, P. Baillon, A.H. Ball, D. Barney, C. Bernet⁵, G. Bianchi, P. Bloch, A. Bocci, A. Bonato, H. Breuker, T. Camporesi, G. Cerminara, T. Christiansen, J.A. Coarasa Perez, D. D'Enterria, A. Dabrowski, A. De Roeck, S. Di Guida, M. Dobson, N. Dupont-Sagorin, A. Elliott-Peisert, B. Frisch, W. Funk, G. Georgiou, M. Giffels, D. Gigi, K. Gill, D. Giordano, M. Giunta, F. Glege, R. Gomez-Reino Garrido, P. Govoni, S. Gowdy, R. Guida, M. Hansen, P. Harris, C. Hartl, J. Harvey, B. Hegner, A. Hinzmann, V. Innocente, P. Janot, K. Kaadze, E. Karavakis, K. Kousouris, P. Lecoq, Y.-J. Lee, P. Lenzi, C. Lourenço, T. Mäki, M. Malberti, L. Malgeri, M. Mannelli, L. Masetti, F. Meijers, S. Mersi, E. Meschi, R. Moser, M.U. Mozer, M. Mulders, P. Musella, E. Nesvold, M. Nguyen, T. Orimoto, L. Orsini, E. Palencia Cortezon, E. Perez, A. Petrilli, A. Pfeiffer, M. Pierini, M. Pimiä, D. Piparo, G. Polese, L. Quertenmont, A. Racz, W. Reece, J. Rodrigues Antunes, G. Rolandi³³, T. Rommerskirchen, C. Rovelli³⁴, M. Rovere, H. Sakulin, F. Santanastasio, C. Schäfer, C. Schwick, I. Segoni, S. Sekmen, A. Sharma, P. Siegrist, P. Silva, M. Simon, P. Sphicas³⁵, D. Spiga, M. Spiropulu³, M. Stoye, A. Tsiros, G.I. Veres¹⁸, J.R. Vlimant, H.K. Wöhri, S.D. Worm³⁶, W.D. Zeuner

Paul Scherrer Institut, Villigen, Switzerland

W. Bertl, K. Deiters, W. Erdmann, K. Gabathuler, R. Horisberger, Q. Ingram, H.C. Kaestli, S. König, D. Kotlinski, U. Langenegger, F. Meier, D. Renker, T. Rohe, J. Sibille³⁷

Institute for Particle Physics, ETH Zurich, Zurich, Switzerland

L. Bäni, P. Bortignon, M.A. Buchmann, B. Casal, N. Chanon, Z. Chen, A. Deisher, G. Dissertori, M. Dittmar, M. Dünser, J. Eugster, K. Freudenreich, C. Grab, D. Hits, P. Lecomte, W. Lustermann, A.C. Marini, P. Martinez Ruiz del Arbol, N. Mohr, F. Moortgat, C. Nägeli³⁸, P. Nef, F. Nessi-Tedaldi, F. Pandolfi, L. Pape, F. Pauss, M. Peruzzi, F.J. Ronga, M. Rossini, L. Sala, A.K. Sanchez, A. Starodumov³⁹, B. Stieger, M. Takahashi, L. Tauscher[†], A. Thea, K. Theofilatos, D. Treille, C. Urscheler, R. Wallny, H.A. Weber, L. Wehrli

Universität Zürich, Zurich, Switzerland

E. Aguilo, C. AMSler, V. Chiochia, S. De Visscher, C. Favaro, M. Ivova Rikova, B. Millan Mejias, P. Otiougova, P. Robmann, H. Snoek, S. Tuppusti, M. Verzetti

National Central University, Chung-Li, Taiwan

Y.H. Chang, K.H. Chen, C.M. Kuo, S.W. Li, W. Lin, Z.K. Liu, Y.J. Lu, D. Mekterovic, A.P. Singh, R. Volpe, S.S. Yu

National Taiwan University (NTU), Taipei, Taiwan

P. Bartalini, P. Chang, Y.H. Chang, Y.W. Chang, Y. Chao, K.F. Chen, C. Dietz, U. Grundler, W.-S. Hou, Y. Hsiung, K.Y. Kao, Y.J. Lei, R.-S. Lu, D. Majumder, E. Petrakou, X. Shi, J.G. Shiu, Y.M. Tzeng, X. Wan, M. Wang

Cukurova University, Adana, Turkey

A. Adiguzel, M.N. Bakirci⁴⁰, S. Cerci⁴¹, C. Dozen, I. Dumanoglu, E. Eskut, S. Girgis, G. Gokbulut, E. Gurpinar, I. Hos, E.E. Kangal, G. Karapinar, A. Kayis Topaksu, G. Onengut, K. Ozdemir, S. Ozturk⁴², A. Polatoz, K. Sogut⁴³, D. Sunar Cerci⁴¹, B. Tali⁴¹, H. Topakli⁴⁰, L.N. Vergili, M. Vergili

Middle East Technical University, Physics Department, Ankara, Turkey

I.V. Akin, T. Aliev, B. Bilin, S. Bilmis, M. Deniz, H. Gamsizkan, A.M. Guler, K. Ocalan, A. Ozpineci, M. Serin, R. Sever, U.E. Surat, M. Yalvac, E. Yildirim, M. Zeyrek

Bogazici University, Istanbul, Turkey

E. Gülmez, B. Isildak⁴⁴, M. Kaya⁴⁵, O. Kaya⁴⁵, S. Ozkorucuklu⁴⁶, N. Sonmez⁴⁷

Istanbul Technical University, Istanbul, Turkey

K. Cankocak

National Scientific Center, Kharkov Institute of Physics and Technology, Kharkov, Ukraine

L. Levchuk

University of Bristol, Bristol, United Kingdom

F. Bostock, J.J. Brooke, E. Clement, D. Cussans, H. Flacher, R. Frazier, J. Goldstein, M. Grimes, G.P. Heath, H.F. Heath, L. Kreczko, S. Metson, D.M. Newbold³⁶, K. Nirunpong, A. Poll, S. Senkin, V.J. Smith, T. Williams

Rutherford Appleton Laboratory, Didcot, United Kingdom

L. Basso⁴⁸, K.W. Bell, A. Belyaev⁴⁸, C. Brew, R.M. Brown, D.J.A. Cockerill, J.A. Coughlan, K. Harder, S. Harper, J. Jackson, B.W. Kennedy, E. Olaiya, D. Petyt, B.C. Radburn-Smith, C.H. Shepherd-Themistocleous, I.R. Tomalin, W.J. Womersley

Imperial College, London, United Kingdom

R. Bainbridge, G. Ball, R. Beuselinck, O. Buchmuller, D. Colling, N. Cripps, M. Cutajar, P. Dauncey, G. Davies, M. Della Negra, W. Ferguson, J. Fulcher, D. Futyan, A. Gilbert, A. Guneratne Bryer, G. Hall, Z. Hatherell, J. Hays, G. Iles, M. Jarvis, G. Karapostoli, L. Lyons, A.-M. Magnan, J. Marrouche, B. Mathias, R. Nandi, J. Nash, A. Nikitenko³⁹, A. Papageorgiou, J. Pela⁴, M. Pesaresi, K. Petridis, M. Pioppi⁴⁹, D.M. Raymond, S. Rogerson, A. Rose, M.J. Ryan, C. Seez, P. Sharp[†], A. Sparrow, A. Tapper, M. Vazquez Acosta, T. Virdee, S. Wakefield, N. Wardle, T. Whyntie

Brunel University, Uxbridge, United Kingdom

M. Chadwick, J.E. Cole, P.R. Hobson, A. Khan, P. Kyberd, D. Leggat, D. Leslie, W. Martin, I.D. Reid, P. Symonds, L. Teodorescu, M. Turner

Baylor University, Waco, USA

K. Hatakeyama, H. Liu, T. Scarborough

The University of Alabama, Tuscaloosa, USA

C. Henderson, P. Rumerio

Boston University, Boston, USA

A. Avetisyan, T. Bose, C. Fantasia, A. Heister, J. St. John, P. Lawson, D. Lazic, J. Rohlf, D. Sperka, L. Sulak

Brown University, Providence, USA

J. Alimena, S. Bhattacharya, D. Cutts, A. Ferapontov, U. Heintz, S. Jabeen, G. Kukartsev, G. Landsberg, M. Luk, M. Narain, D. Nguyen, M. Segala, T. Sinthuprasith, T. Speer, K.V. Tsang

University of California, Davis, Davis, USA

R. Breedon, G. Breto, M. Calderon De La Barca Sanchez, S. Chauhan, M. Chertok, J. Conway, R. Conway, P.T. Cox, J. Dolen, R. Erbacher, M. Gardner, R. Houtz, W. Ko, A. Kopecky, R. Lander, O. Mall, T. Miceli, R. Nelson, D. Pellett, B. Rutherford, M. Searle, J. Smith, M. Squires, M. Tripathi, R. Vasquez Sierra

University of California, Los Angeles, Los Angeles, USA

V. Andreev, D. Cline, R. Cousins, J. Duris, S. Erhan, P. Everaerts, C. Farrell, J. Hauser, M. Ignatenko, C. Jarvis, C. Plager, G. Rakness, P. Schlein[†], J. Tucker, V. Valuev, M. Weber

University of California, Riverside, Riverside, USA

J. Babb, R. Clare, M.E. Dinardo, J. Ellison, J.W. Gary, F. Giordano, G. Hanson, G.Y. Jeng⁵⁰, H. Liu, O.R. Long, A. Luthra, H. Nguyen, S. Paramesvaran, J. Sturdy, S. Sumowidagdo, R. Wilken, S. Wimpenny

University of California, San Diego, La Jolla, USA

W. Andrews, J.G. Branson, G.B. Cerati, S. Cittolin, D. Evans, F. Golf, A. Holzner, R. Kelley, M. Lebourgeois, J. Letts, I. Macneill, B. Mangano, S. Padhi, C. Palmer, G. Petrucciani, M. Pieri, M. Sani, V. Sharma, S. Simon, E. Sudano, M. Tadel, Y. Tu, A. Vartak, S. Wasserbaech⁵¹, F. Würthwein, A. Yagil, J. Yoo

University of California, Santa Barbara, Santa Barbara, USA

D. Barge, R. Bellan, C. Campagnari, M. D'Alfonso, T. Danielson, K. Flowers, P. Geffert, J. Incandela, C. Justus, P. Kalavase, S.A. Koay, D. Kovalskyi, V. Krutelyov, S. Lowette, N. Mccoll, V. Pavlunin, F. Rebassoo, J. Ribnik, J. Richman, R. Rossin, D. Stuart, W. To, C. West

California Institute of Technology, Pasadena, USA

A. Apresyan, A. Bornheim, Y. Chen, E. Di Marco, J. Duarte, M. Gataullin, Y. Ma, A. Mott, H.B. Newman, C. Rogan, V. Timciuc, P. Traczyk, J. Veverka, R. Wilkinson, Y. Yang, R.Y. Zhu

Carnegie Mellon University, Pittsburgh, USA

B. Akgun, R. Carroll, T. Ferguson, Y. Iiyama, D.W. Jang, Y.F. Liu, M. Paulini, H. Vogel, I. Vorobiev

University of Colorado at Boulder, Boulder, USA

J.P. Cumalat, B.R. Drell, C.J. Edelmaier, W.T. Ford, A. Gaz, B. Heyburn, E. Luiggi Lopez, J.G. Smith, K. Stenson, K.A. Ulmer, S.R. Wagner

Cornell University, Ithaca, USA

L. Agostino, J. Alexander, A. Chatterjee, N. Eggert, L.K. Gibbons, B. Heltsley, W. Hopkins, A. Khukhunaishvili, B. Kreis, N. Mirman, G. Nicolas Kaufman, J.R. Patterson, A. Ryd, E. Salvati, W. Sun, W.D. Teo, J. Thom, J. Thompson, J. Vaughan, Y. Weng, L. Winstrom, P. Wittich

Fairfield University, Fairfield, USA

D. Winn

Fermi National Accelerator Laboratory, Batavia, USA

S. Abdullin, M. Albrow, J. Anderson, L.A.T. Bauerdick, A. Beretvas, J. Berryhill, P.C. Bhat, I. Bloch, K. Burkett, J.N. Butler, V. Chetluru, H.W.K. Cheung, F. Chlebana, V.D. Elvira, I. Fisk, J. Freeman, Y. Gao, D. Green, O. Gutsche, A. Hahn, J. Hanlon, R.M. Harris, J. Hirschauer, B. Hooberman, S. Jindariani, M. Johnson, U. Joshi, B. Kilminster, B. Klima, S. Kunori, S. Kwan, C. Leonidopoulos, D. Lincoln, R. Lipton, L. Lueking, J. Lykken, K. Maeshima, J.M. Marraffino, S. Maruyama, D. Mason, P. McBride, K. Mishra, S. Mrenna, Y. Musienko⁵², C. Newman-Holmes, V. O'Dell, O. Prokofyev, E. Sexton-Kennedy, S. Sharma, W.J. Spalding, L. Spiegel, P. Tan, L. Taylor, S. Tkaczyk, N.V. Tran, L. Uplegger, E.W. Vaandering, R. Vidal, J. Whitmore, W. Wu, F. Yang, F. Yumiceva, J.C. Yun

University of Florida, Gainesville, USA

D. Acosta, P. Avery, D. Bourilkov, M. Chen, S. Das, M. De Gruttola, G.P. Di Giovanni, D. Dobur, A. Drozdetskiy, R.D. Field, M. Fisher, Y. Fu, I.K. Furic, J. Gartner, J. Hugon, B. Kim, J. Konigsberg, A. Korytov, A. Kropivnitskaya, T. Kypreos, J.F. Low, K. Matchev, P. Milenovic⁵³, G. Mitselmakher, L. Muniz, R. Remington, A. Rinkevicius, P. Sellers, N. Skhirtladze, M. Snowball, J. Yelton, M. Zakaria

Florida International University, Miami, USA

V. Gaultney, L.M. Lebolo, S. Linn, P. Markowitz, G. Martinez, J.L. Rodriguez

Florida State University, Tallahassee, USA

J.R. Adams, T. Adams, A. Askew, J. Bochenek, J. Chen, B. Diamond, S.V. Gleyzer, J. Haas, S. Hagopian, V. Hagopian, M. Jenkins, K.F. Johnson, H. Prosper, V. Veeraraghavan, M. Weinberg

Florida Institute of Technology, Melbourne, USA

M.M. Baarmand, B. Dorney, M. Hohlmann, H. Kalakhety, I. Vodopyanov

University of Illinois at Chicago (UIC), Chicago, USA

M.R. Adams, I.M. Anghel, L. Apanasevich, Y. Bai, V.E. Bazterra, R.R. Betts, I. Bucinskaite, J. Callner, R. Cavanaugh, C. Dragoiu, O. Evdokimov, L. Gauthier, C.E. Gerber, S. Hamdan, D.J. Hofman, S. Khalatyan, F. Lacroix, M. Malek, C. O'Brien, C. Silkworth, D. Strom, N. Varelas

The University of Iowa, Iowa City, USA

U. Akgun, E.A. Albayrak, B. Bilki⁵⁴, W. Clarida, F. Duru, S. Griffiths, J.-P. Merlo, H. Mermerkaya⁵⁵, A. Mestvirishvili, A. Moeller, J. Nachtman, C.R. Newsom, E. Norbeck, Y. Onel, F. Ozok, S. Sen, E. Tiras, J. Wetzel, T. Yetkin, K. Yi

Johns Hopkins University, Baltimore, USA

B.A. Barnett, B. Blumenfeld, S. Bolognesi, D. Fehling, G. Giurgiu, A.V. Gritsan, Z.J. Guo, G. Hu, P. Maksimovic, S. Rappoccio, M. Swartz, A. Whitbeck

The University of Kansas, Lawrence, USA

P. Baringer, A. Bean, G. Benelli, O. Grachov, R.P. Kenny Iii, M. Murray, D. Noonan, S. Sanders, R. Stringer, G. Tinti, J.S. Wood, V. Zhukova

Kansas State University, Manhattan, USA

A.F. Barfuss, T. Bolton, I. Chakaberia, A. Ivanov, S. Khalil, M. Makouski, Y. Maravin, S. Shrestha, I. Svintradze

Lawrence Livermore National Laboratory, Livermore, USA

J. Gronberg, D. Lange, D. Wright

University of Maryland, College Park, USA

A. Baden, M. Boutemour, B. Calvert, S.C. Eno, J.A. Gomez, N.J. Hadley, R.G. Kellogg, M. Kirn, T. Kolberg, Y. Lu, M. Marionneau, A.C. Mignerey, K. Pedro, A. Peterman, A. Skuja, J. Temple, M.B. Tonjes, S.C. Tonwar, E. Twedt

Massachusetts Institute of Technology, Cambridge, USA

G. Bauer, J. Bendavid, W. Busza, E. Butz, I.A. Cali, M. Chan, V. Dutta, G. Gomez Ceballos, M. Goncharov, K.A. Hahn, Y. Kim, M. Klute, W. Li, P.D. Luckey, T. Ma, S. Nahn, C. Paus, D. Ralph, C. Roland, G. Roland, M. Rudolph, G.S.F. Stephans, F. Stöckli, K. Sumorok, K. Sung, D. Velicanu, E.A. Wenger, R. Wolf, B. Wyslouch, S. Xie, M. Yang, Y. Yilmaz, A.S. Yoon, M. Zanetti

University of Minnesota, Minneapolis, USA

S.I. Cooper, P. Cushman, B. Dahmes, A. De Benedetti, G. Franzoni, A. Gude, J. Haupt, S.C. Kao, K. Klapoetke, Y. Kubota, J. Mans, N. Pastika, R. Rusack, M. Sasseville, A. Singovsky, N. Tambe, J. Turkewitz

University of Mississippi, University, USA

L.M. Cremaldi, R. Kroeger, L. Perera, R. Rahmat, D.A. Sanders

University of Nebraska-Lincoln, Lincoln, USA

E. Avdeeva, K. Bloom, S. Bose, J. Butt, D.R. Claes, A. Dominguez, M. Eads, P. Jindal, J. Keller, I. Kravchenko, J. Lazo-Flores, H. Malbouisson, S. Malik, G.R. Snow

State University of New York at Buffalo, Buffalo, USA

U. Baur, A. Godshalk, I. Iashvili, S. Jain, A. Kharchilava, A. Kumar, S.P. Shipkowski, K. Smith

Northeastern University, Boston, USA

G. Alverson, E. Barberis, D. Baumgartel, M. Chasco, J. Haley, D. Nash, D. Trocino, D. Wood, J. Zhang

Northwestern University, Evanston, USA

A. Anastassov, A. Kubik, N. Mucia, N. Odell, R.A. Ofierzynski, B. Pollack, A. Pozdnyakov, M. Schmitt, S. Stoynev, M. Velasco, S. Won

University of Notre Dame, Notre Dame, USA

L. Antonelli, D. Berry, A. Brinkerhoff, M. Hildreth, C. Jessop, D.J. Karmgard, J. Kolb, K. Lannon, W. Luo, S. Lynch, N. Marinelli, D.M. Morse, T. Pearson, R. Ruchti, J. Slaunwhite, N. Valls, M. Wayne, M. Wolf

The Ohio State University, Columbus, USA

B. Bylsma, L.S. Durkin, A. Hart, C. Hill, R. Hughes, K. Kotov, T.Y. Ling, D. Puigh, M. Rodenburg, C. Vuosalo, G. Williams, B.L. Winer

Princeton University, Princeton, USA

N. Adam, E. Berry, P. Elmer, D. Gerbaudo, V. Halyo, P. Hebda, J. Hegeman, A. Hunt, E. Laird, D. Lopes Pegna, P. Lujan, D. Marlow, T. Medvedeva, M. Mooney, J. Olsen, P. Piroué, X. Quan, A. Raval, H. Saka, D. Stickland, C. Tully, J.S. Werner, A. Zuranski

University of Puerto Rico, Mayaguez, USA

J.G. Acosta, E. Brownson, X.T. Huang, A. Lopez, H. Mendez, S. Oliveros, J.E. Ramirez Vargas, A. Zatserklyaniy

Purdue University, West Lafayette, USA

E. Alagoz, V.E. Barnes, D. Benedetti, G. Bolla, D. Bortoletto, M. De Mattia, A. Everett, Z. Hu, M. Jones, O. Koybasi, M. Kress, A.T. Laasanen, N. Leonardo, V. Maroussov, P. Merkel,

D.H. Miller, N. Neumeister, I. Shipsey, D. Silvers, A. Svyatkovskiy, M. Vidal Marono, H.D. Yoo, J. Zablocki, Y. Zheng

Purdue University Calumet, Hammond, USA

S. Guragain, N. Parashar

Rice University, Houston, USA

A. Adair, C. Boulahouache, V. Cuplov, K.M. Ecklund, F.J.M. Geurts, B.P. Padley, R. Redjimi, J. Roberts, J. Zabel

University of Rochester, Rochester, USA

B. Betchart, A. Bodek, Y.S. Chung, R. Covarelli, P. de Barbaro, R. Demina, Y. Eshaq, A. Garcia-Bellido, P. Goldenzweig, Y. Gotra, J. Han, A. Harel, S. Korjenevski, D.C. Miner, D. Vishnevskiy, M. Zielinski

The Rockefeller University, New York, USA

A. Bhatti, R. Ciesielski, L. Demortier, K. Goulios, G. Lungu, S. Malik, C. Mesropian

Rutgers, the State University of New Jersey, Piscataway, USA

S. Arora, A. Barker, J.P. Chou, C. Contreras-Campana, E. Contreras-Campana, D. Duggan, D. Ferencek, Y. Gershtein, R. Gray, E. Halkiadakis, D. Hidas, A. Lath, S. Panwalkar, M. Park, R. Patel, V. Rekovic, A. Richards, J. Robles, K. Rose, S. Salur, S. Schnetzer, C. Seitz, S. Somalwar, R. Stone, S. Thomas

University of Tennessee, Knoxville, USA

G. Cerizza, M. Hollingsworth, S. Spanier, Z.C. Yang, A. York

Texas A&M University, College Station, USA

R. Eusebi, W. Flanagan, J. Gilmore, T. Kamon⁵⁶, V. Khotilovich, R. Montalvo, I. Osipenkov, Y. Pakhotin, A. Perloff, J. Roe, A. Safonov, T. Sakuma, S. Sengupta, I. Suarez, A. Tatarinov, D. Toback

Texas Tech University, Lubbock, USA

N. Akchurin, J. Damgov, P.R. Duderov, C. Jeong, K. Kovitanggoon, S.W. Lee, T. Libeiro, Y. Roh, I. Volobouev

Vanderbilt University, Nashville, USA

E. Appelt, D. Engh, C. Florez, S. Greene, A. Gurrola, W. Johns, C. Johnston, P. Kurt, C. Maguire, A. Melo, P. Sheldon, B. Snook, S. Tuo, J. Velkovska

University of Virginia, Charlottesville, USA

M.W. Arenton, M. Balazs, S. Boutle, B. Cox, B. Francis, J. Goodell, R. Hirosky, A. Ledovskoy, C. Lin, C. Neu, J. Wood, R. Yohay

Wayne State University, Detroit, USA

S. Gollapinni, R. Harr, P.E. Karchin, C. Kottachchi Kankanamge Don, P. Lamichhane, A. Sakharov

University of Wisconsin, Madison, USA

M. Anderson, M. Bachtis, D. Belknap, L. Borrello, D. Carlsmith, M. Cepeda, S. Dasu, L. Gray, K.S. Grogg, M. Grothe, R. Hall-Wilton, M. Herndon, A. Hervé, P. Klabbers, J. Klukas, A. Lanaro, C. Lazaridis, J. Leonard, R. Loveless, A. Mohapatra, I. Ojalvo, G.A. Pierro, I. Ross, A. Savin, W.H. Smith, J. Swanson

†: Deceased

1: Also at National Institute of Chemical Physics and Biophysics, Tallinn, Estonia

- 2: Also at Universidade Federal do ABC, Santo Andre, Brazil
- 3: Also at California Institute of Technology, Pasadena, USA
- 4: Also at CERN, European Organization for Nuclear Research, Geneva, Switzerland
- 5: Also at Laboratoire Leprince-Ringuet, Ecole Polytechnique, IN2P3-CNRS, Palaiseau, France
- 6: Also at Suez Canal University, Suez, Egypt
- 7: Also at Zewail City of Science and Technology, Zewail, Egypt
- 8: Also at Cairo University, Cairo, Egypt
- 9: Also at Fayoum University, El-Fayoum, Egypt
- 10: Also at Ain Shams University, Cairo, Egypt
- 11: Now at British University, Cairo, Egypt
- 12: Also at Soltan Institute for Nuclear Studies, Warsaw, Poland
- 13: Also at Université de Haute-Alsace, Mulhouse, France
- 14: Now at Joint Institute for Nuclear Research, Dubna, Russia
- 15: Also at Moscow State University, Moscow, Russia
- 16: Also at Brandenburg University of Technology, Cottbus, Germany
- 17: Also at Institute of Nuclear Research ATOMKI, Debrecen, Hungary
- 18: Also at Eötvös Loránd University, Budapest, Hungary
- 19: Also at Tata Institute of Fundamental Research - HECR, Mumbai, India
- 20: Also at University of Visva-Bharati, Santiniketan, India
- 21: Also at Sharif University of Technology, Tehran, Iran
- 22: Also at Isfahan University of Technology, Isfahan, Iran
- 23: Also at Shiraz University, Shiraz, Iran
- 24: Also at Plasma Physics Research Center, Science and Research Branch, Islamic Azad University, Teheran, Iran
- 25: Also at Facoltà Ingegneria Università di Roma, Roma, Italy
- 26: Also at Università della Basilicata, Potenza, Italy
- 27: Also at Università degli Studi Guglielmo Marconi, Roma, Italy
- 28: Also at Università degli studi di Siena, Siena, Italy
- 29: Also at University of Bucharest, Faculty of Physics, Bucuresti-Magurele, Romania
- 30: Also at Faculty of Physics of University of Belgrade, Belgrade, Serbia
- 31: Also at University of Florida, Gainesville, USA
- 32: Also at University of California, Los Angeles, Los Angeles, USA
- 33: Also at Scuola Normale e Sezione dell' INFN, Pisa, Italy
- 34: Also at INFN Sezione di Roma; Università di Roma "La Sapienza", Roma, Italy
- 35: Also at University of Athens, Athens, Greece
- 36: Also at Rutherford Appleton Laboratory, Didcot, United Kingdom
- 37: Also at The University of Kansas, Lawrence, USA
- 38: Also at Paul Scherrer Institut, Villigen, Switzerland
- 39: Also at Institute for Theoretical and Experimental Physics, Moscow, Russia
- 40: Also at Gaziosmanpasa University, Tokat, Turkey
- 41: Also at Adiyaman University, Adiyaman, Turkey
- 42: Also at The University of Iowa, Iowa City, USA
- 43: Also at Mersin University, Mersin, Turkey
- 44: Also at Ozyegin University, Istanbul, Turkey
- 45: Also at Kafkas University, Kars, Turkey
- 46: Also at Suleyman Demirel University, Isparta, Turkey
- 47: Also at Ege University, Izmir, Turkey
- 48: Also at School of Physics and Astronomy, University of Southampton, Southampton, United Kingdom

49: Also at INFN Sezione di Perugia; Università di Perugia, Perugia, Italy

50: Also at University of Sydney, Sydney, Australia

51: Also at Utah Valley University, Orem, USA

52: Also at Institute for Nuclear Research, Moscow, Russia

53: Also at University of Belgrade, Faculty of Physics and Vinca Institute of Nuclear Sciences, Belgrade, Serbia

54: Also at Argonne National Laboratory, Argonne, USA

55: Also at Erzincan University, Erzincan, Turkey

56: Also at Kyungpook National University, Daegu, Korea